


Advanced Materials / Volume 36, Issue 7 / 2306772

Review |  Full Access

## Low-Dimensional-Materials-Based Photodetectors for Next-Generation Polarized Detection and Imaging

Wei Xin, Weiheng Zhong, Yujie Shi, Yimeng Shi, Jiawei Jing, Tengfei Xu, Jiaxiang Guo, Weizhen Liu, Yuanzheng Li, Zhongzhu Liang, Xing Xin , Jinluo Cheng , Weida Hu , Haiyang Xu , Yichun Liu

First published: 04 September 2023

<https://doi-org-ssl.hanyang.sjlib.cn/10.1002/adma.202306772>

Citations: 3

[Find It @ Hanyang](#)

---

### Abstract

The vector characteristics of light and the vectorial transformations during its transmission lay a foundation for polarized photodetection of objects, which broadens the applications of related detectors in complex environments. With the breakthrough of low-dimensional materials (LDMs) in optics and electronics over the past few years, the combination of these novel LDMs and traditional working modes is expected to bring new development opportunities in this field. Here, the state-of-the-art progress of LDMs, as polarization-sensitive components in polarized photodetection and even the imaging, is the main focus, with emphasis on the relationship between traditional working principle of polarized photodetectors (PPs) and photoresponse mechanisms of LDMs. Particularly, from the view of constitutive equations, the existing works are reorganized, reclassified, and reviewed. Perspectives on the opportunities and challenges are also discussed. It is hoped that this work can provide a more general overview in the use of LDMs in this field, sorting out the way of related devices for “more than Moore” or even the “beyond Moore” research.

### 1 Introduction

Visual inputs play a crucial role in how humans perceive the external environment, which drives our long-term obsession of the information acquisition of light.<sup>[1, 2]</sup> From a large perspective, light is an electromagnetic wave that contains several fundamental elements such as intensity, wavelength, phase and polarization, while only the intensity within a limited range of wavelengths ( $\approx 390\text{--}760\text{ nm}$ ) can be interpreted by us without the help of external aids.<sup>[2, 3]</sup> In the past few decades, people have gradually realized the importance of multielement extraction of light. More extraction will provide us with more opportunities to understand the world.

Unlike the first three scalar elements of light mentioned above, the polarization has vector characteristics. Since human eyes do not have the ability to extract this vector information directly, it is of great significance to compensate this defect by developing polarized photodetection equipment containing advanced optical and computational science. Indeed, the idea of designing polarized photodetectors (PPs) has already been proposed since the early 1970s.<sup>[4, 5]</sup> After more than 50 years of development, the portable equipment with high resolution and real-time response characteristics has been widely used in various fields, such as astronomical observation, remote sensing, clinical and biomedicine, quantum physics and so on.<sup>[6-9]</sup> **Figure 1** summarizes the development history of PPs briefly.<sup>[10-27]</sup> It can be seen that at early stages the prepared equipment usually requires complex optical path at the expense of compact volume to spatially separate the different polarization state information of the imaging target. This dilemma is not changed until the rise of micro/nano-optoelectronics. By integrating many functions in space, the PPs have made the leap from "equipment" to "devices." Especially since the low-dimensional materials (LDMs) have been widely concerned in the last decades, combing traditional working modes of PPs with novel LDMs is expected to impetus this field to a new level of research.<sup>[19-27]</sup>

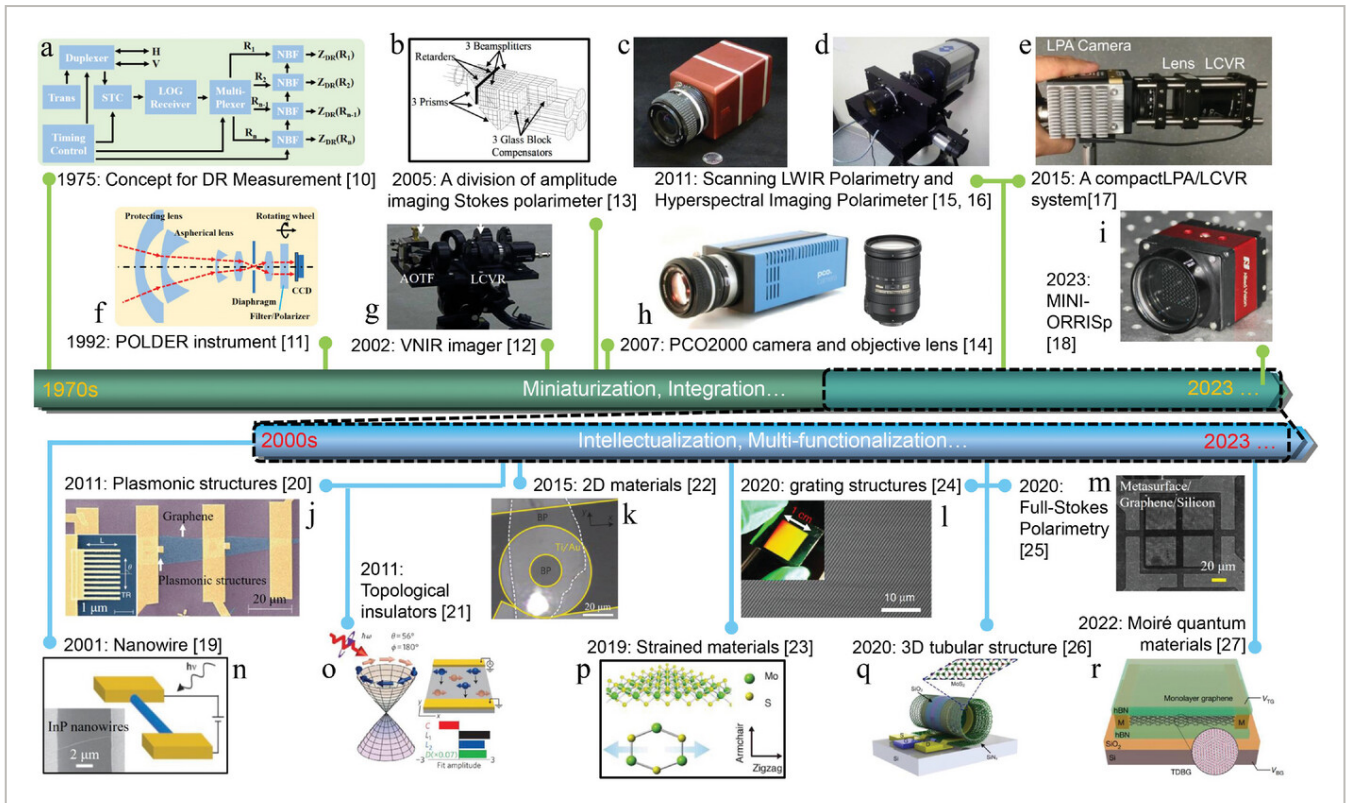


**Figure 1**

[Open in figure viewer](#) | [PowerPoint](#)

The development roadmap of PPs, with emphasis on the applications of LDMs in this field since 2000. Reproduced with permission.<sup>[10-27]</sup> a) Reproduced with permission.<sup>[10]</sup> Copyright 1976, American Meteorological Society. b) Reproduced with permission.<sup>[13]</sup> Copyright 2005, SPIE. c) Reproduced with permission.<sup>[15]</sup> Copyright 2011, SPIE. d) Reproduced with permission.<sup>[16]</sup> Copyright 2011, OSA Publishing. e) Reproduced with permission.<sup>[17]</sup> Copyright 2017, OSA Publishing. f) Reproduced with permission.<sup>[11]</sup> Copyright 1993, Elsevier. g) Reproduced with permission.<sup>[12]</sup> Copyright 2002, SPIE. h) Reproduced with permission.<sup>[14]</sup> Copyright 2007, SPIE. i) Reproduced with permission.<sup>[18]</sup> Copyright 2023, SPIE. j) Reproduced with permission.<sup>[20]</sup> Copyright 2011, Springer Nature. k) Reproduced with permission.<sup>[22]</sup> Copyright 2015, Springer Nature. l) Reproduced under the terms of the CC-BY Creative Commons Attribution 4.0 International license (<https://creativecommons.org/licenses/by/4.0>).<sup>[24]</sup> Copyright 2020, The Authors, published by Springer Nature. m) Reproduced with permission.<sup>[25]</sup> Copyright 2020, American Chemical Society. n) Reproduced with permission.<sup>[19]</sup> Copyright 2001, American Association for the Advancement of Science. o) Reproduced with permission.<sup>[21]</sup> Copyright 2011, Springer Nature. p) Reproduced with permission.<sup>[23]</sup> Copyright 2019, Elsevier. q) Reproduced under the terms of the CC-BY Creative Commons Attribution 4.0 International license (<https://creativecommons.org/licenses/by/4.0>).<sup>[26]</sup> Copyright 2020, The Authors, published by de Gruyter. r) Reproduced with permission.<sup>[27]</sup> Copyright 2022, Springer Nature.

In contrast to the morphology of bulk materials, the volumes of LDMs are usually constrained within a limited space, formulating the types such as 2D materials, 1D nanotubes/wires, or 0D quantum dots, etc.<sup>[28-32]</sup> Recently, with continuous development in

material preparation and processing, LDMs also show diversification in shape. For example, the quantum dots/nanotubes in a Russian-doll type or the nanoribbons, -meshes, -cones with other special morphologies have appeared one after another.<sup>[32-34]</sup> Sometimes the size of the LDM does not need to be confined to the atomic level if we want to highlight certain aspects of the device functions.<sup>[35, 36]</sup>

Generally speaking, LDMs exhibit the advantages in photodetection as follow:

First, the sub- or nanometer size in the geometry of LDM results in an insufficient Coulomb screening, which leads to a strong quantum confinement enhancement and forms much stable hydrogen-like bound electron-hole pairs (so-called excitons). This is the basis for LDMs to have strong light-matter interactions. Accordingly, LDMs present remarkable linear/nonlinear optical responses, high-efficiency hot carriers transport and ultrafast charge/energy transfer rates.<sup>[37-42]</sup> Second, LDMs are easy to be composited or integrated with other materials because of the rich morphology and small size. Both the energy bands and interfaces can be engineered easily. On the one hand, due to the abundant energy band structures, suitable LDMs can be selected to regulate the spectral response range of devices by composing the homo/heterogeneous junctions.<sup>[43-45]</sup> On the other hand, the high specific areas of LDMs highlight the influence on the properties by the surface defect states or the local fields.<sup>[46, 47]</sup> It makes the photodetectors more advantageous in many aspects, including response spectrum (UV-THz), response speed (>GHz), detectivity ( $>10^{10}$  Jones), room-temperature operation, than those of their bulk counterparts.<sup>[48-50]</sup> Third, LDMs present intrinsic abilities to identify linearly/chiral polarized light, showing high polarization selectivity which is an important factor in PPs. By constructing the junctions, or combining LDMs with fibers, resonators, waveguides, metasurfaces or other structures, the LDMs-based PPs (LDPPs) exhibit extremely high extinction ratios, which may overcome the problems caused by the signal crosstalk or bulky volume in traditional device structures.<sup>[51, 52]</sup> Benefiting from these advantages, developing LDPPs is expected to be effective to push traditional PPs to miniaturization, integration, multifunctionalization and intellectualization in the future (Figure 1).

In this review, we pay more attention to the pivotal role of LDMs as photoelectric conversion units in PPs, mainly focusing on the polarization mechanism, state-of-the-art research progress, and the challenges and opportunities. Although there exist reviews on polarized optoelectronic properties of LDMs and their corresponding applications, most of them are usually limited to a selected type of LDMs and lack a systematic description of polarized photodetection from a more focused perspective. Besides, the relationship between traditional working principle of PPs and polarized photoresponse mechanisms of LDPPs is also discussed insufficiently, which confuses the classification of existing devices. Therefore, it is necessary to reorganize and review the existing works in detail.

Different from the previous reports, to systematically understand the mechanisms for the polarized photoresponse of LDPPs, we start with the discussion of constitutive relation with

the inclusion of nonlinear terms first. The electric fields  $E(t)$  can be written as<sup>[53-55]</sup>

$$E(t) = E_{dc} + E_1(\omega) e^{-i\omega t} + E_1^*(\omega) e^{i\omega t} \quad (1)$$

where  $E_{dc}$  is the static electric field corresponding to the direct current (dc), and  $E_1(\omega)$  is the light field at circular frequency  $\omega$ . The static current density  $J_{dc}^i$  can be written as

$$J_{dc}^i = \sigma_{dc}^{(1);ij}(0) E_{dc}^j + 2\sigma^{(2);ikm}(\omega, -\omega) E_1^k (E_1^m)^* + 6\sigma^{(3);ijkm}(0, \omega, -\omega) E_{dc}^j E_1^k (E_1^m)^* + \dots \quad (2)$$

Here, the  $\sigma_{dc}^{(1);ij}(0)$ ,  $\sigma^{(2);ikm}(\omega, -\omega)$ , and  $\sigma^{(3);ijkm}(0, \omega, -\omega)$  are dc conductivity, second-order conductivity and third-order conductivity tensors, respectively. The subscripts  $i, j, k, m = \{x, y, z\}$  represent the Cartesian coordinates.

Furthermore, we can abbreviate the Equation (2) as

$$\begin{aligned} J_{dc}^i &= \sigma_{dc}^{(1);ij}(0) E_{dc}^j + 2\sigma^{(2);ikm}(\omega, -\omega) E_1^k (E_1^m)^* \\ &\quad + 6\sigma^{(3);ijkm}(0, \omega, -\omega) E_{dc}^j E_1^k (E_1^m)^* + \dots \\ &= \left[ \sigma_{dc}^{(1);ij}(0) + 6\sigma^{(3);ijkm}(0, \omega, -\omega) E_1^k (E_1^m)^* \right] E_{dc}^j \\ &\quad + 2\sigma^{(2);ikm}(\omega, -\omega) E_1^k (E_1^m)^* + \dots \\ &= \left[ \sigma_{dc}^{(1)} + \Delta\sigma^{(1)} \right] E_{dc}^j + \sigma^{(2)} EE + \dots \\ &= \sigma^{(1)} E^{(1)} + \sigma^{(2)} EE + \dots \end{aligned} \quad (3)$$

Under light illumination, the current changes in Equation (3) come from the latter two terms, which are fully determined by the nonlinear conductivities tensors  $\sigma^{(2)}$  and  $\sigma^{(3)}$ . When these components show anisotropy for different direction of the dc field and light field,  $\Delta J_{dc}^i = \Delta\Delta\sigma^{(1)} \cdot E_{dc}^j + \sigma^{(2)} EE + \dots = \Delta\sigma\Delta E \cdot E_{dc}^j + \sigma^{(2)} EE + \dots$ , the detectors can achieve a specific response to polarized light.

Based on the origin of currents, the LDPPs can be divided into three classes: the type of anisotropic linear photoconductivity ( $\Delta\sigma$ ), anisotropic photoexcitation ( $\Delta E$ ) and high-order nonlinear photoresponse ( $\sigma^{(2)}EE$ , type I, II and III for short, See Section 4 for more details). This classification can effectively take into consideration the vast majority of existing devices. After that, we introduce the state-of-the-art works, mainly focusing on their performance comparisons between different type of devices. At last, the challenges and opportunities, as well as the perspectives currently faced in this field are listed. We hope this review can provide beneficial reference to the development of LDPPs.

## 2 Polarized Photodetection Mechanism

Practical usage of LDMs in PPs requires the following three points to be sorted out in order: the working principle of PPs, photoresponse mechanisms of LDMs, and physical basis for their polarization-dependent characteristics. This chapter will mainly discuss from these three points.

### 2.1 Working Principle of PPs

Light is a transverse electromagnetic wave in free space, which propagates orthogonally to both directions of electric field and magnetic field. For any light beam, its polarization state can be described mainly by four interchangeable representations: trigonometric function, H-Poincaré sphere, Jones calculus, and Stokes calculus. Among them, the Stokes calculus attracts more attention due to its explicit description of the polarization states of light and convenient extraction in experiments by the full Stokes measurement.<sup>[2, 3, 54]</sup> In brief, here we assume that the light travels in  $z$  direction and we decompose it into a vector superposition of two linear polarized light perpendicular to each other ( $x$  and  $y$  directions with amplitudes of  $E_{0x}$  and  $E_{0y}$ ) with a fixed phase difference  $\chi$ . Then, we can define the Stokes vector  $(S_0, S_1, S_2, S_3)^T$  with four Stokes components as follows (**Figure 2a**)

$$\begin{pmatrix} S_0 \\ S_1 \\ S_2 \\ S_3 \end{pmatrix} = \begin{pmatrix} I \\ Q \\ U \\ V \end{pmatrix} = \begin{pmatrix} E_{0x}^2 + E_{0y}^2 \\ E_{0x}^2 - E_{0y}^2 \\ 2E_{0x}E_{0y}\cos\chi \\ 2E_{0x}E_{0y}\sin\chi \end{pmatrix} \propto \begin{pmatrix} I_0 + I_{90} \\ I_0 - I_{90} \\ I_{45} + I_{135} \\ I_L - I_R \end{pmatrix} \quad (4)$$

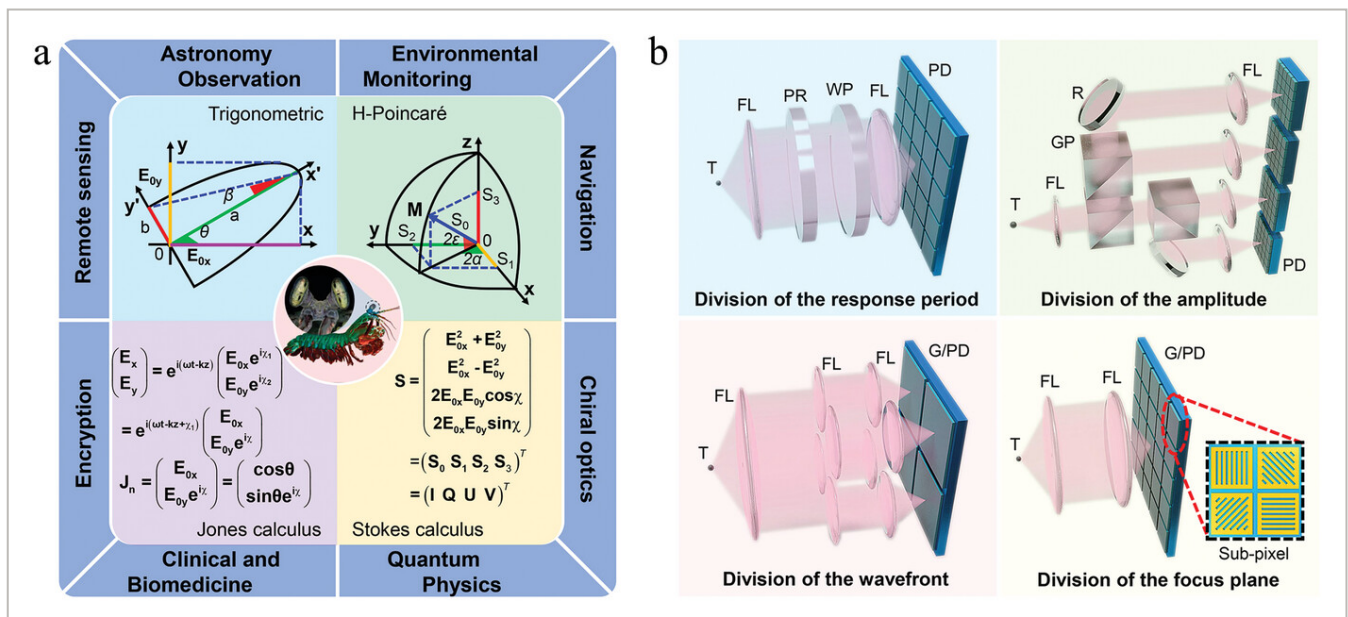


Figure 2

a) Different descriptions of vector characteristics of light and the applications of related PPs in different areas. The center depicts a mantis shrimp with compound eyes, which has the ability to detect polarized information. b) PPs of different configurations, including the division-of-response period (DRP)/-amplitude (DA)/-wavefront (DW) and -focus plane (DFP) types. The T, FL, R, GP, PR, WP, PD and G represent the target, focus lens, reflector, Gran prism, polarizer, wave plate, photodetector and grating, respectively.

The  $I_0$ ,  $I_{45}$ ,  $I_{90}$ ,  $I_{135}$ ,  $I_L$ , and  $I_{RR}$  here represent the intensities of linear polarized light at different polarization states (the subscript number means the included angle with the x-axis), and the left/right (L/R) circular polarized light intensities, respectively. This vector can completely describe the polarization state of a light. As the light passes through a specific optical element, its vectors before and after the element are connected through a Stokes–Mueller vectorial transformation as  $S_{out} = M \cdot S_{in}$ , and the  $M$  is a  $4 \times 4$  Muller Matrix with real elements.<sup>[3, 54]</sup> Furthermore, based on the four Stokes components, other parameters, such as degree of polarization (DOP), can also be defined, which are usually used for specifically analyzing the polarization characteristics of light (**Table 1** for details).

**Table 1.** Parameters related to the polarization-dependent characteristics of light

Parameter	Expression <sup>a)</sup>	Value range
Degree of polarization	$DOP = P = \sqrt{S_1^2 + S_2^2 + S_3^2} / S_0$	$0 \leq P \leq 1$
Degree of linear polarization	$DOLP = P_L = \sqrt{S_1^2 + S_2^2} / S_0$	$0 \leq P_L \leq 1$
Degree of circular polarization	$DOCP = P_C = S_3 / S_0$	$0 \leq P_C \leq 1$
Angle of polarization	$AOP = \theta_A = \frac{1}{2} \arctan \frac{S_2}{S_1}$	$-\frac{\pi}{2} \leq \theta_A \leq \frac{\pi}{2}$
Angle of ellipticity	$AOE = \theta_\varepsilon = \frac{1}{2} \arcsin \frac{S_3}{\sqrt{S_1^2 + S_2^2 + S_3^2}}$	$-\frac{\pi}{4} \leq \theta_\varepsilon \leq \frac{\pi}{4}$

a) The  $S_0$ ,  $S_1$ ,  $S_2$ ,  $S_3$  are Stokes parameters related to the intensity of polarized light. See Figure 2a for the specific expressions.

It can be seen from the Equation (4) that the electric field amplitudes ( $E_{0x}$ ,  $E_{0y}$ ) and fixed phase difference  $\chi$  are critical for describing the polarization information of light. And we can also simplify the Stokes components in the vector by arithmetical operations between light intensities of different polarization states, which can be further measured in experiment by a combination of beam splitters, wave plates, polarizers and detectors. For example, suppose that a light from a target passes through a number of optical elements and strikes a detector (Figure 2b). The intensities of light with different polarization states at the image point are easy to measure, so the corresponding Stokes vector ( $S_{out}$ ) and other

polarization information such as DOP are available. By further measuring these spatial-dependent parameters, the imaging of polarization information of a certain scene at its image space is obtained. Since the Mueller matrixes ( $M$ ) are known for the given optical elements, the polarization imaging of the target at the object space ( $S_{in}$ ) can be derived accordingly. Significantly, the  $S_{out}$  and  $S_{in}$  are usually equivalent in experiment, so we can only care about the spatial-dependent  $S_{out}$  in most cases.<sup>[56]</sup>

According to the above idea, different ways have been tried and different configurations of PP systems, including the division-of-response period (DRP)/amplitude (DA)/wavefront (DW) type, have been designed in the past few decades (Figure 2b).<sup>[10-18, 57-61]</sup> However, the PP equipment rather than PP devices are called in these configurations due to the complex optical paths and huge volumes. The compact design of related systems has always been the focus of attention in this field. Examples of the compact model for polarized photodetection can be found in real life as references, such as the visual system of mantis shrimps.<sup>[62, 63]</sup> By considering the compound eyes as vertically stacked photodiodes, it can be found that the crystalline cone, parallel-aligned microvillis and rhabdom cells respectively realize the functions of focusing light spots and filtering, polarization sensitivity and spectral discrimination in a compact space (Figure 2a). Inspired by this, the PPs with division-of-focus plane (DFP) configuration were designed.<sup>[64-66]</sup> The polarization filters and detection elements are effectively integrated together here, pushing the PP “equipment” to “devices.” The LDPPs are mainly developed on this basis. By replacing the traditional probe units with LDMs-based detectors with polarization-dependent characteristics, the integration of the PPs is expected to be further improved. However, a test system in practice should also take into account the hardware optimization, software development and advanced algorithms and so forth. More contents about the device signal calibration and denoising can be found in these references.<sup>[56, 67-70]</sup>

## 2.2 Photoresponse Mechanisms of LDMs

Photoresponse describes processes in a material that convert the incident photons into carriers or currents. Much work has reported on the related mechanisms of LDMs, and the corresponding photodetectors have also been classified as photonic- or thermal-induced types.<sup>[71, 72]</sup> Differently, in this review we classify the mechanisms into linear and nonlinear types based on the constitutive equation, which may reveal the physical consequences of the light excitation in the photoresponse more clearly, and facilitate to clarify differences and establish connections between different types of LDPPs.

Compared with the nonlinear counterpart, the change of linear conductivity under light (photoconductivity,  $\Delta\sigma^{(1)}$ ) of a material is generally more influential in terms of its current generation. From the constitutive equation, the  $\Delta\sigma^{(1)}$  can be understood as



Considering the complex relaxation processes in crystals, the conductivity change can also be understood in a different way: the light induces carrier density changes  $\Delta n$ , which is proportional to the light absorption, or the real part of the photoconductivity  $\text{Re}[\Delta\sigma^{(1)}(\omega)]$ . The additional carrier density leads to the changes of dc conductivity  $\Delta\sigma^{(1)}$  and finally  $\Delta J \approx \Delta\sigma^{(1)}$ . Based on this, numerous mechanisms, such as photoconductive effect (PCE), photogating effect (P-GE), photobolometric effect (PBE), photovoltaic effect (PVE), photothermoelectric effect (PTE) and photo-Dember effect (PDE), etc., are investigated.<sup>[73-76]</sup> The difference is that a bias is required to generate a directional current in the former three processes, while the latter can directly induce the current without an external field, which is dominated by whether a uniform or a space-dependent  $\Delta\sigma^{(1)}$  is caused by the incident light. The type-II band alignment, gradient Seebeck coefficients and carrier diffusion coefficients are key factors in the latter three processes respectively.<sup>[73-76]</sup> On this basis, we can also divide the photodetectors into bias-dependent and zero-bias types, as shown in **Table 2**. Interestingly, on closer inspection at the constitutive equation in our review, we can find that the linear photoconductivity here is actually determined by the product of third-order nonlinear conductivity and light intensity. This does not contradict the description abovementioned, but rather hints at some novel physical processes, such as photocurrents that may analogous to be induced by the Hall effects.

**Table 2.** Photoresponse mechanisms

Type	Mechanism	Description	Expression	Symb
Linear effect- induced mechanisms	Bias- dependent	Photoconductive effect (PCE)	The photon- generated carriers increase the excess concentration and photoconductivity of related materials. A bias voltage is needed to separate the electrons and holes and drive them to different electrodes to form photocurrent.	$\Delta\sigma^{(1)}$ t photo and conc anc ele qua charg chan
		Photogating effect (P-GE) <sup>a)</sup>	After irradiating a material, one type of carriers is trapped in localized states, resulting in an increase in the concentration of another carriers and material conductivity	The P-GE can be considered as a particular case of PCE.

a) To distinguish the photogating effect and photogalvanic effect in expression, we abbreviate the former as P-GE and the latter as PGE here.

In addition to the effects of light on the linear photoconductivity of a material, the second-order nonlinear terms in the constitutive equation is also important for current generation under some circumstances. Here we mainly introduce some representative second-order nonlinear mechanisms, such as photogalvanic effect (PGE), photon drag effect (PDE) and bulk photovoltaic effect (BPVE).<sup>[77-79]</sup> These physical processes can be induced by many factors, but the lattice symmetry of materials and the incident directions and polarization states of light usually need to be considered. As soon as the product of  $(\sigma^{(2)} \cdot EE)$  with third-rank tensors is not zero under certain circumstances, the nonlinear photocurrent without a bias voltage will be generated. To further describe the characteristics of the above mechanisms in detail, the relevant definitions and formulas are summarized in Table 2.

The above mechanisms are universal to most materials, but they may become more obvious in LDMs due to the unique properties such as reduced screening and enhanced quantum confinement.<sup>[80, 81]</sup> Because LDMs are affected by surrounding environment easily, the local symmetry breaking of lattices and interfacial defect states may also lead to interesting photoresponse.<sup>[82, 83]</sup> In addition, it should be noted that the process for generating photocurrents of a material is complex, and the mechanism is by no means limited to the categories described above. For example, the photoelectromagnetic effect, magneto-concentration effect and other effects have also been reported in LDMs-based detectors.<sup>[84-88]</sup> Under some special conditions, multiple mechanisms may combine to cause the photoresponse of a material. Therefore, in most cases only the dominant factors induced in photodetectors are discussed, and the devices should be designed with special configurations to achieve some certain functions.

## 2.3 Polarized Photoresponse Mechanisms of LDPPs

After introducing the mechanisms of LDMs' response to light, it is ready to further discuss the polarized photoresponse origins of related LDPPs. By referring to the above-mentioned constitutive equation, the change in photocurrent density excited by different polarized light can be expressed as

(6)

Then, the mechanisms affecting the polarized performance of existing LDPPs can be divided into three types: the type of anisotropic linear photoconductivity ( $\Delta\sigma$ , type I), anisotropic photoexcitation ( $\Delta E$ , type II) and high-order nonlinear photoresponse ( $\sigma^{(2)} \cdot EE$ , type III) (**Figure 3**).

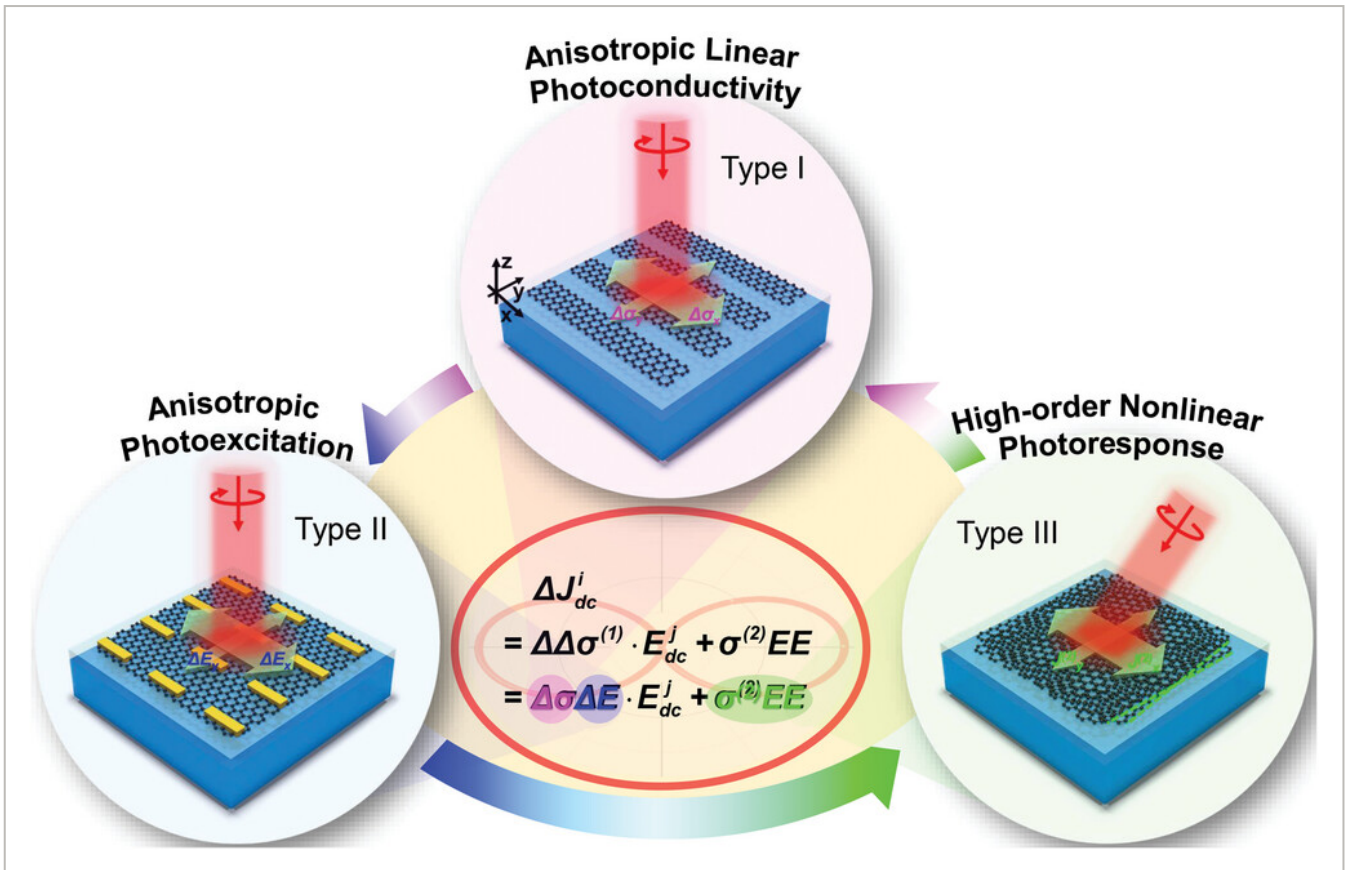


**Figure 3**

[Open in figure viewer](#) | [PowerPoint](#)

Classification of LDPPs from the perspective of constitutive equation.

Type-I LDPPs require a material possesses anisotropic photoconductivities ( $\Delta\sigma$ ) excited by light with different polarization states. For this type, the optical elements to modulate polarization states before the photodetector is not necessary. Taking the black phosphorus (BP) which is a typical anisotropic 2D material as an example, it can exhibit obvious anisotropic optical absorption along its zigzag/armchair directions, and further induce diverse  $\Delta\sigma$  for different light polarizations.<sup>[89, 90]</sup> By contrast, type-II LDPPs focus more on the anisotropic modulation of light field ( $\Delta E$ ) through external factors. For example, when the sub-wavelength grating structures are prepared on the surface of a 2D material, the material may also anisotropic due to the different modulation abilities of these structures on incident electromagnetic waves with different polarization states.<sup>[24, 91]</sup> For better performance, sometimes the type-I and II LDPPs can be realized in one configuration. In addition, the nonlinear effects of LDMs are also significant under some special conditions, which gives rise to the type-III LDPPs. The tensor properties of the nonlinear conductivity naturally lead to the polarization-dependent properties of devices. The detailed descriptions including the principles, state-of-the-art LDPPs and characteristic analysis for each category will be introduced in Sections 8–10.

It should be noted that whether the LDPPs respond to circular or linear polarized light is without discriminating here because in most cases they have similar mechanisms despite of the slightly different influence factors. To avoid duplication, we mainly focus on the response of materials to linear polarized light in this review. The response to circular light of LDMs will be focused on in Section 11.

## 3 PPs Based on LDMs

In this section, we will first introduce the parameters for valuing the performance of photodetectors. And then, the representative LDPPs and their characteristics divided according to the above discussions will be described. Specifically, the LDPPs responded to linear polarized light will be mainly concentrated in Sections 8–10, and the devices response to circular polarized light are focused on in Section 11.

### 3.1 Figures-of-Merit for PPs

There are many parameters to evaluate the performance of photodetectors, and they can be classified into two classes: the intensity-related and sensitivity-related parameters.<sup>[92]</sup> The first class includes parameters such as photoresponsivity ( $R$ ) and on/off ratio ( $R^*$ ), which reflect the photoresponse intensity of a device caused by incident lights. For discrepant working mechanisms, they are defined under a given bias. The  $R$  and  $R^*$  can be defined at zero bias for PV device due to their self-powered characteristics, while a small bias is usually needed for PC detectors. In addition, as two important parameters affecting  $R$  and  $R^*$ , the external quantum efficiency ( $\eta$ , EQE) and photoconductive gain ( $G$ ) are also widely used to characterize the photoresponse intensities of the devices. On the basis of the definition of  $R$  and  $R^*$ , and the formula , where  $I_{ph}$ ,  $\Gamma$  and  $e$  are the photocurrent, number of absorbed photons per unit time and electron charge, it can be found that the higher the quantum efficiency and gain, the higher the optical response.<sup>[93, 94]</sup> The second class includes sensitivity-related parameters, such as the noise equivalent power (NEP), specific detectivity ( $D^*$ ), response/decay time ( $\tau_{rise}/\tau_{fall}$ ), and cut-off frequency ( $f_c$ ), which describes the sensitivity of a detector to the optical environment. The former two parameters describe the ability of a device to detect weak signals, while the latter ones reflect the response speed to an optical pulse. Significantly, most of these parameters are wavelength-dependent, so they need to be discussed at a certain spectral band.

Apart from the above parameters usually concerned in conventional photodetectors, another critical parameter for PPs is the anisotropic ratio ( $\delta$ ).<sup>[19]</sup> Although there are different expressions in literature, it is uniformly expressed as the ratio between the maximal and minimal photocurrent ( $I_{max}/I_{min}$ ) caused by different polarized light here to facilitate the performance comparison between different devices.  $\delta$  is directly related to the ability of PPs to resolve the polarization information. The larger the value, the larger the extinction ratio of the device, and the better the device can distinguish the information differences. Taking the calculation of DOLP as an example, if the anisotropic ratio of a device is reduced from 100 to

10, its polarization information resolution will be reduced by  $\approx 17\%$  accordingly. A device with high  $\delta$  is more likely to obtain the polarization information of object which is less susceptible to environmental interference. To obtain a polarized image with ideal spatial resolution ( $>0.8$  of DOLP for instance), the anisotropy ratio generally needs to be larger than 10 in practice.

In order to further describe the characteristics of the above parameters, the definitions and expressions are summarized in **Table 3** in detail. It should be noted that there is no unified standard for measuring the above parameters of LDMS-based photodetectors for a long time, which leads to the performance deviations between the actual values and the reported ones. Just recently, Hu's group has systematically introduced how to characterize the figures of merit of 2D photodetectors, which can also be a reference for measuring other LDMS-based devices.<sup>[95]</sup>

**Table 3.** Key figures-of-merit for PPs

Type	Parameter/Units	Expression	Description
Intensity-related parameters	Photoresponsivity		$R$ is defined as the ratio of the photocurrent ( $I_{ph}$ ) to the power of incident light ( $P$ ). $I_{ph}$ is the current difference of device before and after illumination, shown as .
		$[R, AW^{-1}]$	
	On/Off Ratio		$R^*$ reflects the ratio of photocurrent to dark current.
		$[R^*, -]$	
Sensitivity-related parameters	Photoconductive gain		$G$ evaluates the ability of generating multiple carriers by a single incident photon, where $\tau_{life}$ and $\tau_{tran}$ are the life time and drift transit time of the photogenerated electrons/holes in channel, respectively.
		$[G, -]$	
	External quantum efficiency		$\eta$ is the number ratio of the collected charge carriers to the photons illuminating the device that produce the photocurrent, where $h$ , $c$ , $q$ and $\lambda$ are Planck constant, speed of light, electron charge and wavelength of incident light, respectively.
	$[\eta, -]$		
Sensitivity-related	Noise equivalent power		NEP is the minimum light signal power that can be detected or distinguished from the background. The $NEP$ is the noise current

- a) There are two definitions of anisotropic ratio ( $\delta$ ). In order to ensure the uniformity of full-text data comparison, here we totally describe it as  $I_M/I_m$ . The larger the value, the higher the DOP of the device.

## 3.2 Overview of the Characteristics of Different Types of LDPPs

Among all LDMs, 1D/2D materials with intrinsic in-plane anisotropy have natural advantages in polarized photodetection. Referring to the configurations of conventional DFP-PPs, the large-area, uniform 1D arrays or 2D films are potential materials in device manufacturing.<sup>[96-98]</sup> The anisotropic crystal structure of a material makes its many properties anisotropic, including the linear/nonlinear photoconductivities, carrier mobility and effective mass, etc. This can also be understood by anisotropic selection rules, which is mostly determined by the inversion or mirror reflection symmetry.<sup>[90, 99]</sup> In order to describe such anisotropy in detail, the in-plane conductivities of a material in perpendicular directions ( $\sigma_x, \sigma_y$ ) can be extracted by means of semiclassical Drude model and spectral measurements.<sup>[100, 101]</sup> Then, the absorption coefficient, refractive index, energy loss coefficient, etc. can be obtained accordingly.<sup>[73, 74]</sup> The anisotropic parameters are basis for polarization sensitivity of type-I LDPPs. Thanks to the clear mechanisms involved and simple device configurations, such type has attracted much attention in the past decade. Nevertheless, the intrinsic low anisotropic ratios ( $\delta < 5$ ) and lacking of the ability to detect linear/circular polarized light simultaneously are the main obstacles to further development of them.

Different from type-I LDPPs where the polarization-dependent photoresponse of a LDM is the key ingredient to realize polarized photodetection, type-II LDPPs depend on the regulation of incident light with a specific polarization state. A common feature is to attenuate the light intensity for unwanted polarization component, which can be easily realized by attaching a polarizer before the surface of the photosensitive material. Thus, the optical components with the ability to modulate electromagnetic field performance, such as the metasurfaces, resonators and waveguides etc., are usually added in the type-II LDPPs. Because of the excellent properties and flexible working modes, such device especially the one integrated with metamaterials is considered most promising for practical applications in the future. However, an age-old problem to be solved is the accurate, high-speed fabrication of some certain, refined micro/nanostructures, which is difficult for optical components especially used in the visible or the ultraviolet spectral range.<sup>[102]</sup>

The above two types are developed on the basis of the linear relationship between current density and conductivity/electric field intensity. They are prevailing in polarized photodetection of LDMs at present, while the detectors based on the nonlinear response effects are less studied. These nonlinear phenomena are mainly caused by interaction of the carriers with multiple photons, which leads to a directional transmission of them and a self-driving current without bias voltage. In this case important issues are the material symmetry, polarization states of light, and incident angles. Because the morphologies of

LDMs are affected easily by environment, the symmetry-breaking of substrates and the edge/topological surface states, defects or lattice fluctuations of materials can also result in the nonlinear response.<sup>[82]</sup> This is the basis on which we can apply these effects to type-III LDPPs. They are not limited to the LDMs but can be stronger than their bulk counterparts due to the fire-new induced mechanisms, high nonlinear coefficients and efficient light–matter coupling. These nonlinear interactions bring promise for detectors working in new modes, as shown by the fact that a topological material can be excited to generate photocurrent with photon energies smaller than the bulk band gap.<sup>[103, 104]</sup> However, the weak current signals caused by the inconspicuous nonlinear interactions may usually be drowned out by ambient noises. Meanwhile, due to the relative strict conditions for exciting nonlinear current, how to combine the traditional detection model with existing excitation conditions is also a problem that needs to be considered. These problems set up obstacles for the practical applications of type-III LDPPs in the future.

In addition, it should be noted that 0D materials, mainly including quantum dots, fullerene, nanocrystals, etc., are not mentioned as typical materials in the polarized photodetection in this review. This is mainly because their isotropic lattice structures or disordered distributions make them rarely exhibit polarization-dependent photoresponse, although sometimes their chirality or high-order nonlinearity may play a role.<sup>[105-107]</sup> However, due to their strong quantum confinement, high light absorption, large specific surface area and tunable size-related band structure, etc., great flexibility in device performance regulation has been presented.<sup>[108-110]</sup> More relevant works will be mainly discussed in Section 13.

### 3.3 Type-I LDPPs

1D nanowire or nanotube is one of the most representative materials applied to the type-I LDPPs. Considering the light-matter interaction, 1D materials as a whole exhibit intrinsic anisotropy even though it can have an isotropic lattice at the atomic scale. As early as 2001, Lieber's group has prepared a photodetector based on an isolated 20-nm diameter InP nanowire. The photoresponse can hardly be seen when the polarization direction of light is perpendicular to the wire. Calculated from the Maxwell's equations, the electric field intensities are found attenuated strongly at this moment and the light that parallel to the wire is unaffected, leading to an anisotropic ratio ( $\delta$ ) as high as  $\approx 21$  (**Figure 4a**).<sup>[19]</sup> This work pioneers the polarized photoresponse research of 1D materials. Subsequently a lot of attentions have been paid to them or even their compounds. As an example, Sun's group investigated the polarization dependence of carbon nanotubes in 2015. Under excitation of electromagnetic waves at 2.52 THz, the detector exhibits an anisotropic ratio of  $\approx 1.43$  (**Figure 4b**).<sup>[111]</sup> In recent years, with the rapid development of material preparation and processing, large-area 1D arrays and subwavelength gratings have been fabricated.<sup>[112-114]</sup> They are usually anisotropic as well, which makes them effective complements to photosensitive materials in LDPPs. However, the main factors of polarized photoresponse of these materials are not consistent with changing their diameters. When the diameter is



small enough, the quantum confinement plays a major role in the polarized response; when the diameter increases gradually, the polarization dependence mainly depends on its modulation of the light field. Therefore, the devices in these two different cases should belong to different types, and whether the quantum confinement is obvious is the main criterion to judge. To avoid repetition with previous reports, more 1D materials-based PPs are listed in **Table 4**. The related parameters are also compared for reference.<sup>[19, 24, 91, 111, 115-144]</sup>

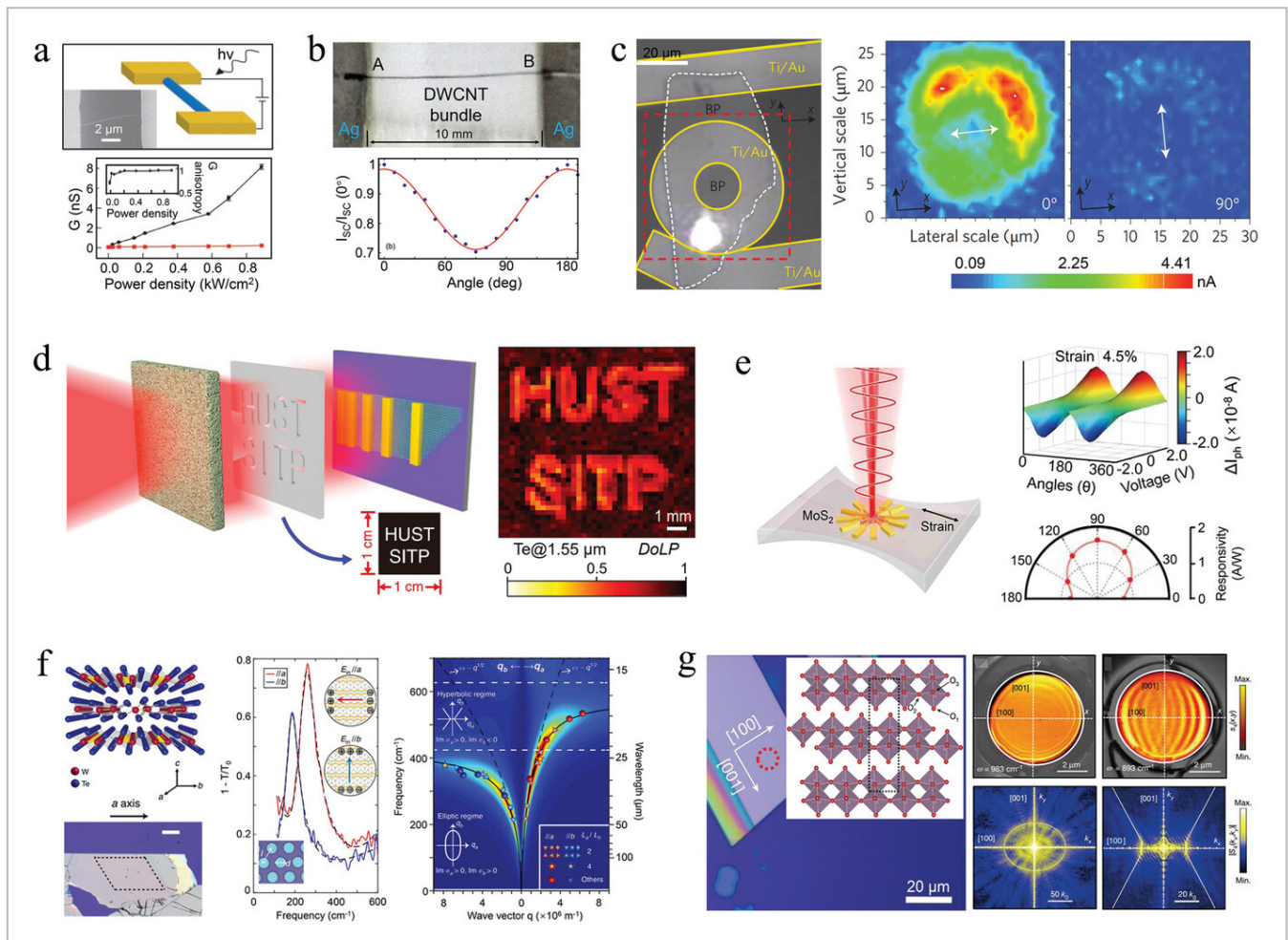


**Figure 4**

[Open in figure viewer](#) | [PowerPoint](#)

Typical examples of type-I LDPPs. a) Schematic, optical picture and anisotropic photoconductive gain of an individual InP nanowire device. b) Optical picture and normalized polarized photoresponse of a double-walled carbon nanotube photodetector. c) Optical image and polarized photocurrent maps of the BP photodetector with a ring-shaped collector. d,e) Schematics and polarization-dependent DoLP image/strain-induced photoresponse of the Te/MoS<sub>2</sub> photodetectors, respectively. f) Schematic, optical picture and the anisotropic extinction spectra, plasmon dispersions of a WTe<sub>2</sub> flake. g) Schematic, optical picture, near-field amplitude images and the corresponding Fourier transform pictures of a MoO<sub>3</sub> disk. a) Reproduced with permission.<sup>[19]</sup> Copyright 2001, American Association for the Advancement of Science. b) Reproduced with permission.<sup>[111]</sup> Copyright 2015, Optica Publishing Group. c) Reproduced with permission.<sup>[22]</sup> Copyright 2015, Springer Nature. d) Reproduced under the terms of the CC-BY Creative Commons Attribution 4.0

International license (<https://creativecommons.org/licenses/by/4.0>).<sup>[174]</sup> Copyright 2020, The Authors, published by Springer Nature. e) Reproduced with permission.<sup>[23]</sup> Copyright 2019, Elsevier. f) Reproduced under the terms of the CC-BY Creative Commons Attribution 4.0 International license (<https://creativecommons.org/licenses/by/4.0>).<sup>[191]</sup> Copyright 2020, The Authors, published by Springer Nature. g) Reproduced with permission.<sup>[192]</sup> Copyright 2018, Springer Nature.

**Table 4.** Performance comparison of 1D-PPs (the 1D-PPs specifically refer to the polarized photodetectors based on 1D materials and their arrays)

Type	Materials	Bandgap [eV]	Response band [nm]	$R$ [ $A W^{-1}$ ]	$\Delta$	Ref.
Nanotube	Double-walled carbon	–	$118.8 \times 10^3$	$1.6 \times 10^{-2}$	1.43	[111]
	Single-walled carbon	0.46	1500	–	177	[115]
Nanowire	InP	–	488/514	3000@514 nm <sup>a)</sup>	21.2	[19]
	GaN	3.4	254	–	1.38	[116]
	CdSe	1.74	350–740	0.3@400 nm	7	[117]
	ZnO	–	514	–	1.16	[118]
	NbN	–	650	–	1.06	[119]
	Ge	0.8	1550	–	1.6	[120]
	ZnTe	2.26	300–500	$1.87 \times 10^5$ @532 nm	3	[121]
	TaS <sub>3</sub>	1.13	532–1097	2500@808 nm	4	[122]
	Nb <sub>(1-x)</sub> Ti <sub>x</sub> S <sub>3</sub>	1.13	200–1400	2978@633 nm	1.75	[123]
	“ ”	“ ”	“ ”	“ ”	“ ”	“ ”

a) The value after the symbol @ represents the specific wavelength associated with the photoresponsivity and anisotropic ratio of the device. Table 5 and Table 6 are also expressed in the same format.

As another kind of representative, in-plane anisotropic 2D materials have also been widely used in type-I LDPPs recently. For example, Cui's group verified the broadband polarization sensitivity of few-layer BP in 2014 (Figure 4c).<sup>[22]</sup> The maximum anisotropic ratio ( $\delta$ ) can reach  $\approx 4$ .<sup>[145-147]</sup> However, the instability of BP in air greatly limits its applications and the

study for substituting it with stable ones is continuing. Up to now, more than 30 kinds of anisotropic 2D materials have been reported and they are mainly concentrated in triclinic, monoclinic and orthorhombic crystal systems.<sup>[148-177]</sup> Their response spectra cover a wide range from ultraviolet to mid-infrared bands. In principle, all of these materials are potential to be used in polarized imaging, but it was not until 2020 that Tong et al. experimentally verified the feasibility with a few-layer Te material (Figure 4d).<sup>[174]</sup> By means of a scanning detection technique, they obtained the polarized image of a designed target by means of the space-dependent DOLP in obscured conditions for the first time. Despite the poor spatial resolution due to the low anisotropy ratio ( $\delta < 8$ ), it greatly pushes the practical applications of anisotropic 2D materials in this field. In addition to the intrinsic materials above-mentioned, the anisotropy can also be designed artificially by applying stress in one direction in the plane of a material to reduce its spatial symmetry. In 2019, Tong et al. observed the polarized photoresponse in an otherwise isotropic monolayer MoS<sub>2</sub> by this method. It also provides a universal scheme for the performance control of PPs (Figure 4e).<sup>[23]</sup> **Table 5** summarize the performance of current 2D materials-based LDPPs in detail.<sup>[148-177]</sup> It can be found that the anisotropic ratio ( $\delta$ ) of these devices are mostly low (usually  $<5$ ), and how to improve the values is still one of the key problems that need to be concerned. Several ways such as preparing composite structures, building van der Waals (vdW) materials or applying local fields have been implemented, and searching for new natural materials with outstanding anisotropic properties is still a hotspot.<sup>[178-181]</sup> To keep systematic of this article, the discussion about modulating device performance will be mainly concentrated in Sections 11 and 13.

**Table 5.** Performance comparison of 2D-PPs (the 2D-PPs specifically refer to the polarized photodetectors based on natural anisotropic 2D materials)

Type	Materials	Bandgap [eV]	Response band [nm]	$R$ [ $\text{AW}^{-1}$ ]	$(\tau_{\text{rise}}/\tau_{\text{fall}}, \mu\text{s})$
Orthorhombic	$\text{CaNb}_2\text{O}_6$	3.85	280–400	–	1000
	$\text{PdPSe}$	1.46	405/808	$5.07 \times 10^3 @ 808$ nm	$0.1/0.44 \times 10^6$
	$\text{SnS}$	1.38	450/638/808/1064/1550	$3.1 \times 10^2 @ 450$ nm	–
	$\text{Sb}_2\text{Se}_3$	1.2	400–1100	$0.18 @ 1050$ nm	$144/96 \times 10^3$
	$\text{GeSe}$	1.1–1.2	400–950	$4.25 @ 808$ nm	–
	$\text{BP}$	0.33	1100–1700	$1.5 \times 10^{-3} @ 1700$ nm	40
	$\text{PdSe}_2$	0.03	300–1100	$14.5 @ 369$ nm	$3.2/3.8 \times 10^6$
	$\text{Ta}_2\text{NiSe}_5$	0.36	400–1064	$44 @ 1064$ nm	$98/82 \times 10^3$

In addition to the above work, the study of photoelectric anisotropy of materials by exciting other quasi-particles, such as plasmons or polaritons, has also attracted a lot of attention recently. The plasmons are known as collective oscillations of electrons, and the polaritons are coupling between photons and phonons in polar materials or photon-exciton hybrids in cavities (phonon/exciton polaritons).<sup>[182-184]</sup> Benefit from the light–matter interaction, the excitation of these particles helps to miniaturize the device sizes, which is significant especially in the infrared and THz bands.<sup>[185-187]</sup> Different from the isotropic counterparts, the anisotropic 2D materials present advantages in directional propagation of these quasi-particles. If the product  $\sigma_x \cdot \sigma_y$  is less than zero in some certain bands, the isofrequency surfaces of extraordinary waves will be reshaped as hyperbolic, further leading to the anisotropic quasi-particles.<sup>[188-190]</sup> For example, in 2020 Wang et al. first observed the anisotropic plasmons and their elliptic–hyperbolic transitions in  $\text{WTe}_2$  films (Figure 4f).<sup>[191]</sup> A little earlier, the anisotropic polaritons in natural  $\alpha\text{-MoO}_3$  were also observed by Ma et al. (Figure 4g).<sup>[192]</sup> Interestingly, by designing and patterning the nanostructures on the surface of some 2D materials, the transport behavior of these quasi-particles can be further

governed.<sup>[193, 194]</sup> In 2022, Zhang et al. experimentally observed the extremely asymmetric and unidirectional excitation of polaritons in  $\alpha$ -MoO<sub>3</sub> flakes with blazed nanograting structures, which presents important potential in on-chip photonics.<sup>[194]</sup> Despite of significant progress, great challenges remain if these quasi-particles are excited for photodetection in practice. The first thing that needs to be considered is how to make these particles work in traditional light paths rather than just observe or modulate them in the near field. Exciting hybrid modes in specific device configurations is proven effective.<sup>[195-197]</sup> Second, finding easier methods to match momentum between the incident light and plasmons/polaritons is another critical issue in the development of this field.<sup>[197-200]</sup> Although enormous difficulties may be faced, the attractive properties of anisotropic 2D materials still make them promising for polarized photodetection.

### 3.4 Type-II LDPPs

Different from the intrinsic anisotropy of LDMs in type-I LDPPs, the polarization-dependent photoresponse of type-II LDPPs is mainly caused by the modulation of light field of LDMs by external factors. One kind of representative devices are based on the 1D material arrays or subwavelength grating structures prepared on the surface of 2D material films. Here, the quantum confinement and quasi-particles excitation (plasmons/polaritons) are not required. The polarized photoresponse of LDMs only depends on the limited transmission, reflection and diffraction of electromagnetic wave in the structures. The parameters such as the anisotropic equivalent refractive indexes ( $n_x$ ,  $n_y$ ) are usually introduced to describe this process.<sup>[201, 202]</sup> In 2017, Jiang's group prepared the 1D perovskite single-crystal arrays with strict orders by using a solution-processing method.<sup>[91]</sup> The average width of these 1D arrays is about 510 nm and the largest anisotropic ratio can be 2.6 (**Figure 5a**). In another work, Zou et al. prepared the high-quality graphene grating films with  $\approx$ 780 nm period by using a femtosecond laser plasmonic lithography technique (**Figure 5b**).<sup>[24]</sup> By further optimizing the morphology parameters, the devices realized tunable polarized photoresponse and birefringent in the visible band.<sup>[203]</sup>

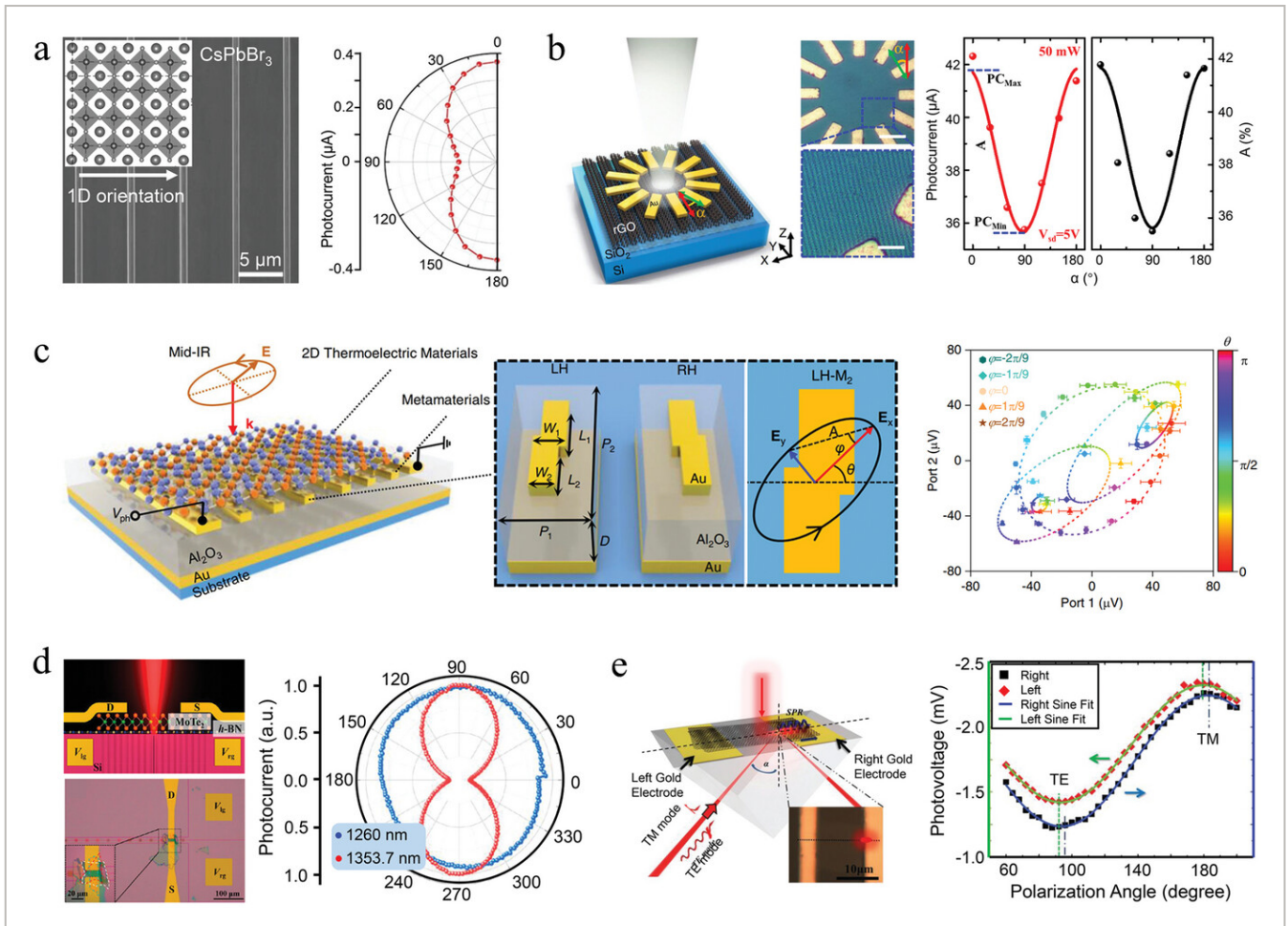


**Figure 5**

[Open in figure viewer](#) | [PowerPoint](#)

Representative studies of type-II LDPPs. a,b) Schematics, optical pictures and polarization-dependent photocurrents/optical absorption of the 1D perovskite nanowire arrays/ graphene nanogratings. c) Schematic and full-Stokes polarimetry of a photodetector integrated with the 2D thermoelectric material and chiral metamaterials. d,e) Schematics, optical image and polarization-dependent photocurrent/photovoltage of a photonic-crystal-cavity integrated MoTe<sub>2</sub> photodetector/twisted bilayer graphene in total reflection mode. a) Reproduced with permission.<sup>[91]</sup> Copyright 2017, Wiley-VCH. b) Reproduced under the terms of the CC-BY Creative Commons Attribution 4.0 International license (<https://creativecommons.org/licenses/by/4.0>).<sup>[24]</sup> Copyright 2020, The Authors, published by Springer Nature. c) Reproduced under the terms of the CC-BY Creative Commons Attribution 4.0 International license (<https://creativecommons.org/licenses/by/4.0>).<sup>[209]</sup> Copyright 2022, The Authors, published by Springer Nature. d) Reproduced with permission.<sup>[213]</sup> Copyright 2021, American Chemical Society. e) Reproduced with permission.<sup>[217]</sup> Copyright 2016, Wiley-VCH.

In addition to the device configurations mentioned above, combining LDMs with periodic micro/nanostructures is also effective to implement type-II LDPPs. Ever since Powell et al. confirmed the plasmons on metal surface and their abilities for selectively transmitting light with different polarization states in the last century, great enthusiasm has been devoted to

replacing traditional polarizers and making them widely available for polarized photodetection.<sup>[204-206]</sup> For example, in 1999 Nordin et al. prepared a Mo grating with  $\approx 475$  nm period on a Si substrate and it presented an anisotropic ratio ( $\delta$ ) of  $\approx 1000$  at 3–5  $\mu\text{m}$ .<sup>[207]</sup> After integrated it into an infrared camera, the device can realize polarized imaging of a static scene clearly, which offers a universal solution for similar applications of LDMs.<sup>[52]</sup> However, with the development of electromagnetic field theory and processing technology, people prefer the combination of metamaterials and LDMs because the latter one presents much richer configurations and more flexible optical field regulation ability.<sup>[208]</sup> In 2020, Wang's group constructed a graphene/Si photodetector composed of  $2 \times 2$  units. By optimizing the morphologies of Au structures on each unit, the device can both distinguish the linear and circular polarized light with different polarization states simultaneously.<sup>[25]</sup> In 2022, by designing metamaterials on the  $\text{PdSe}_2$ , Dai et al. also realized the polarized photoresponse, successfully obtaining the full-Stokes imaging of objects in the infrared range (Figure 5c).<sup>[209]</sup>

Thanks to the flexibility of type-II LDPPs in regulating electromagnetic fields, not only metamaterials but also other components such as resonators, photonic crystals and fibers can integrate with LDMs for polarized photodetection.<sup>[210-212]</sup> Here, another two representative device configurations are introduced. First, in 2021 Li et al. prepared a  $\text{MoTe}_2$  photodetector that is constructed on a silicon photonic crystal (Figure 5d). Due to the different coupling efficiency of radiation into the cavity, a polarized photoresponse with maximum anisotropic ratio ( $\delta$ ) of 11.5 was demonstrated.<sup>[213-215]</sup> Unfortunately, it is hard to maintain high performance in a wide range limited by the working principle of such devices. Second, LDMs can also exhibit anisotropic response to light in the total internal reflection mode because of the discrepant complex refractive indexes in and out of the 2D plane (RI ellipsoid). In 2015, Tian's group first described the properties of a monolayer and twisted-bilayer graphene in this configuration (Figure 5d), respectively.<sup>[216, 217]</sup> A reversed anisotropic ratio can be achieved on a large scale just by tuning the incident angle of light and the direction of incidence plane.<sup>[218]</sup>

### 3.5 Type-III LDPPs

In this section, the representative type-III LDPPs based on second-order nonlinear effects such as PGE, PDE and BPVE are mainly introduced.<sup>[77, 78]</sup> As one of the most well-known ones, PGE was first predicted in bulk materials as early as 1970s.<sup>[219, 220]</sup> With the rapid development of materials science recently, it has been observed in many LDMs, such as nanoparticles, nanotubes/wires, 2D topological insulators, type-II Weyl semimetals, transition metal dichalcogenides (TMDs), etc., and has been developed into a tool for selectively resolving the band spin splitting, spin-valley coupling, and Berry curvature singularities.<sup>[107, 221-227]</sup> PGE describes the asymmetrical scattering of carriers by light to generate directional net current in a material. It can only occur in a crystal without inversion symmetry in the dipole interaction approximation. As the interaction between light and

electric quadrupole and magnetic dipole is considered, the symmetry limitation can be removed but an oblique incidence of light is mostly required in LDMs. For example, Král et al. first carried out a theoretical study on the PGE of BN nanotubes. The tubes with different chiral numbers may have intrinsic noncentrosymmetric (NCS) and their polar properties are proven helpful to excite the shift currents (**Figure 6a**).<sup>[223]</sup> In 2011, McIver et al. experimentally observed a surface current in a  $\text{Bi}_2\text{Se}_3$ . Due to the Dirac band structures and the counter-propagating fermions with opposite spins in this topological insulator material, a net current was induced when the spins were selectively driven, resulting in a circular polarization-dependent photoresponse at a certain oblique angle (circular PGE, CPGE).<sup>[21]</sup> Similar phenomena were also observed by Agarwal et al. in a  $\text{WTe}_2$  flake in 2020.<sup>[228]</sup> By designing the electrodes with U-shaped geometries and exciting the topological surface charge with a polarized Laguerre–Gaussian beam, the orbital angular momentum /energy-electrons transfer process is revealed (Figure 6b).<sup>[228, 229]</sup>

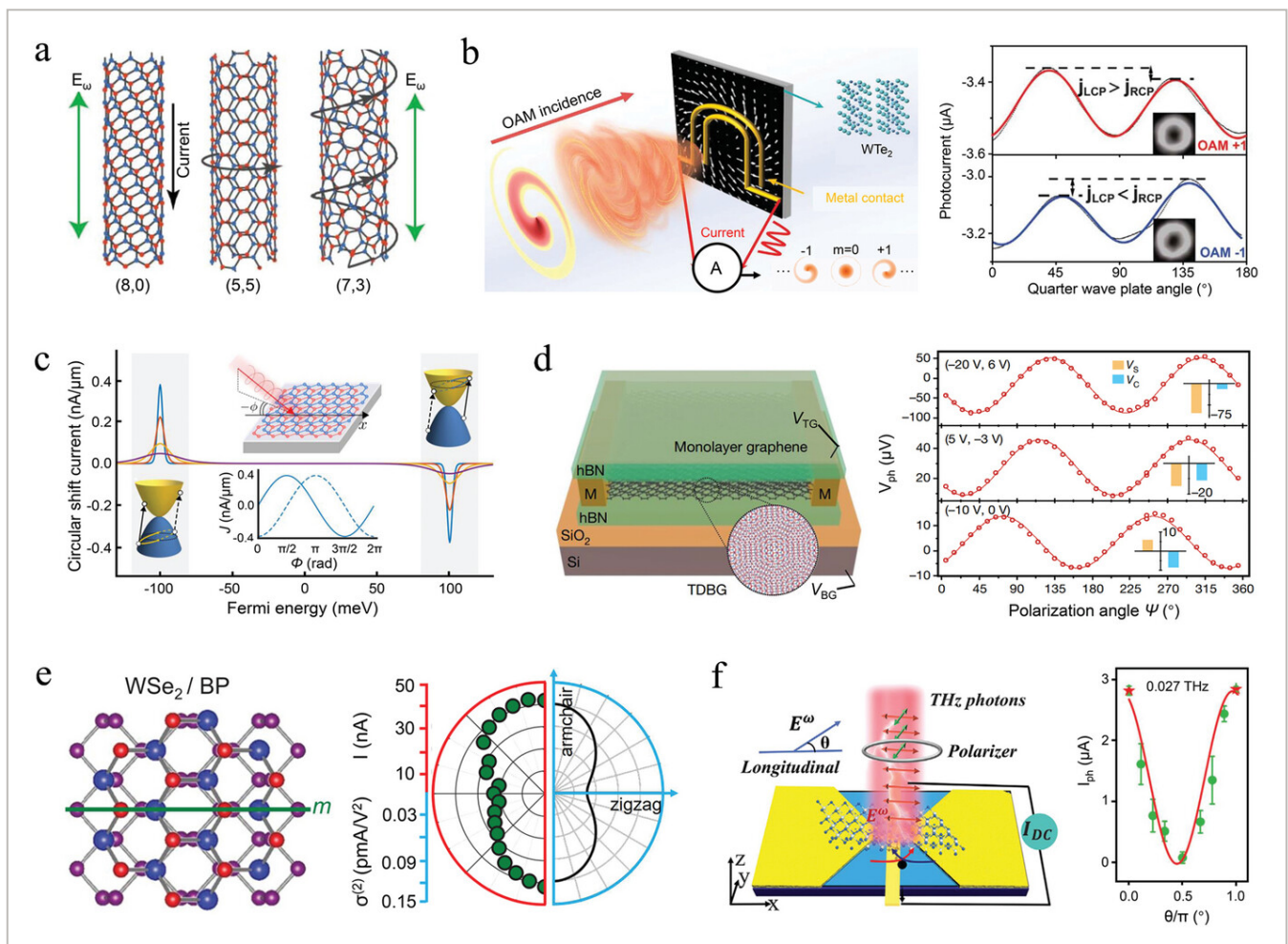


**Figure 6**

[Open in figure viewer](#) | [PowerPoint](#)

Typical examples of the type-III LDPPs. a) Theoretical predicted shift currents of different curled BN nanotubes along their axis. b) Schematic and polarization-dependent current of a  $\text{WTe}_2$  flake induced by orbital angular momentum of light. c) Schematic and calculated circular shift photocurrent of a bilayer graphene. d–f) Schematics and the



corresponding polarization-dependent photovoltages/nonlinear conductivity/photocurrent of devices made of twisted double bilayer graphene/WSe<sub>2</sub>-BP heterojunction/1T-CoTe<sub>2</sub> flake, respectively. a) Reproduced with permission.<sup>[223]</sup> Copyright 2000, American Physical Society. b) Reproduced with permission.<sup>[228]</sup> Copyright 2020, American Association for the Advancement of Science. c) Reproduced with permission.<sup>[238]</sup> Copyright 2022, American Physical Society. d) Reproduced with permission.<sup>[27]</sup> Copyright 2022, Springer Nature. e) Reproduced with permission.<sup>[244]</sup> Copyright 2021, American Association for the Advancement of Science. f) Reproduced with permission.<sup>[245]</sup> Copyright 2023, Wiley-VCH.

Another well-known nonlinear optical effect is PDE, which is generally described as the momentum transfer from photons to electrons.<sup>[78]</sup> Unlike PGE that can only be observed in NCS materials, PDE is intrinsic and commonly presented in any conductors. Since the effect was first predicted in bulks in the 1950s, this nonlinear phenomenon has been observed experimentally in a variety of materials.<sup>[230-233]</sup> Over the past decade, the research of PDE has also been extended to LDMs. In 2010, Entin et al. discussed the PD current in graphene considering the resonant/nonresonant mechanisms.<sup>[234]</sup> When graphene is excited near the Fermi energy, a small shift in momentum may lead to a strong difference in relaxation times between carriers, further inducing an increased net current. This process has been widely agreed upon and validated in carbon nanotubes and TI materials subsequently.<sup>[235, 236]</sup> In recent years, another model was proposed to describe the PDE by Xiong et al.<sup>[237]</sup> They attributed the current to a shift dipole, namely the geometrically nonvertical optical transitions between interbands. Only the electron Bloch states below the Fermi energy were excited. So the carriers with opposite wave vectors were selectively driven to generate a directional net current. This process is not limited by the symmetry of material and it is demonstrated in a bilayer graphene system later (Figure 6c).<sup>[238]</sup>

Apart from the PGE and PDE, BPVE has also caught much attention in LDMs in recent years, which is potential to be induced in the NCS materials with piezoelectric/ferroelectric properties.<sup>[239]</sup> Microscopically, BPVE is determined by the asymmetric scattering centers of a material as well. This is similar to that in PGE, so mostly they are viewed equally. BPVE can also be used as the basis for polarized photodetection.<sup>[107]</sup> For example, Peng et al. explored the photocurrent in a 2D perovskite and confirmed the key role of BPVE both with the temperature-related and zero-bias experiments in 2020.<sup>[240]</sup> Similar phenomena were also observed in  $\alpha$ -In<sub>2</sub>Se<sub>3</sub>, BiFeO<sub>3</sub>, Td-WTe<sub>2</sub> and so on.<sup>[241-243]</sup> In 2022, the BPVE in a twisted double bilayer graphene (TDBG) has sparked renewed interest. Both the symmetry breaking and moiré quantum geometry are considered. By introducing the convolutional neural networks, the authors even realized the full-Stokes polarimetry in LDMs based on the BPVE for the first time (Figure 6d).<sup>[27]</sup>

Some other second-order nonlinear effects also have been studied recently. In 2021, Akamatsu et al. designed a WSe<sub>2</sub>/BP photodetector and revealed the role of spontaneous photovoltaic effect. By controlling the lattice symmetry between WSe<sub>2</sub> and BP, a polarization-dependent zero-bias current of the system was observed (Figure 6e).<sup>[244]</sup> In another work,

Hu et al. explored the nonlinear Hall effect of CoTe<sub>2</sub> flakes in the THz range. Interestingly, a current conversion by rectifying the driving alternating current were realized in the absence of a magnetic field (Figure 6f).<sup>[245]</sup>

### 3.6 Circular Polarized Photoresponse of LDMs

The response mechanisms of LDMs to linear polarized light and the classifications for related devices are also applicable to circular light–matter interactions. Generally, the physical process can still be analyzed from the view of linear conductivity, electric field intensity and nonlinear conductivity tensor terms in the constitutive equation, but the difference is the definition conversion from linear to circular polarized light. In order to be consistent with previous statements, the LDPPs response to circular polarized light are also divided into three categories: type I, II, and III respectively. A brief description of each type and the typical examples are given.

The materials involved in type-I LDPPs usually include small molecules, polymers, organic single crystals, perovskites and so on.<sup>[105, 106, 246-248]</sup> Generally, these materials are chiral intrinsically for recognizing the polarization states of circular light and can be made into 0D hybrids, 1D nanowires, 2D thin films or even their composites. In 2013, Campbell's group prepared a field-effect transistor that was capable of resolving circular light by using a 1-aza-[6]helicene molecular.<sup>[249]</sup> Thanks to the natural helical structures, a maximum anisotropic ratio  $\approx 10$  at turn-on voltage was obtained (**Figure 7a**). By extending the chirality of material, namely the  $\pi$ -conjugation, along its helix or in-plane direction, the chirality dependence will be more pronounced.<sup>[250]</sup> As an example, by connecting  $\pi$ -conjugated naphthalene skeleton with (PbI<sub>6</sub>)<sup>4-</sup> chains in a perovskite nanowire, Ishii et al. fabricated a detector with highest anisotropic ratio of  $\approx 25.4$  in 2020 (Figure 7b).<sup>[251]</sup> Although the extinction performances of these PP are better than their linear-polarized-light-responded counterparts, great progress are still needed for practical applications. In contrast, the type-II LDPPs are much more vigorous in this respect because of the rich devices configurations. The controllable photoresponse to circular polarized light can be realized easily by integrating the LDMs with metamaterial units.<sup>[252, 253]</sup> Recently, by constructing the metamaterials on the surface of a few-layered MoS<sub>2</sub> and introducing the concept of “optoelectronic silent state,” Bu et al. achieved a response with ultrahigh extinction ratio to the circular polarized light, which further laid the foundation for the practical application of LDMs.<sup>[254]</sup> Compared with the above two categories, the type-III LDPPs is furthest away from applications at the present stage because of the relative weak photoresponse and low compatibility with optical paths of traditional PPs. Many researches in this field are still focused on the property explorations of novel materials.<sup>[77]</sup> For example, in 2018 Paul et al. experimentally demonstrated the helicity-dependent photocurrent driven by the spin Hall mechanism at the edge of a Bi<sub>2</sub>Te<sub>2</sub>Se platelet, while the phenomenon can only be temporarily stayed in the laboratory due to the distance from the requirements of polarized photodetection in practice.<sup>[255]</sup> In order to solve above problems, Qiu's group recently proposed a new strategy: they

constructed the periodic asymmetric metal micro-nano/structures on the surface of graphene, and stimulated the BPVE of the material through near-field optical regulation to generate the net current. Unlike most of the type-II LDPPs, the photocurrent excited here exhibits distinct vector characteristics, so it can flow without external bias.<sup>[256-258]</sup>

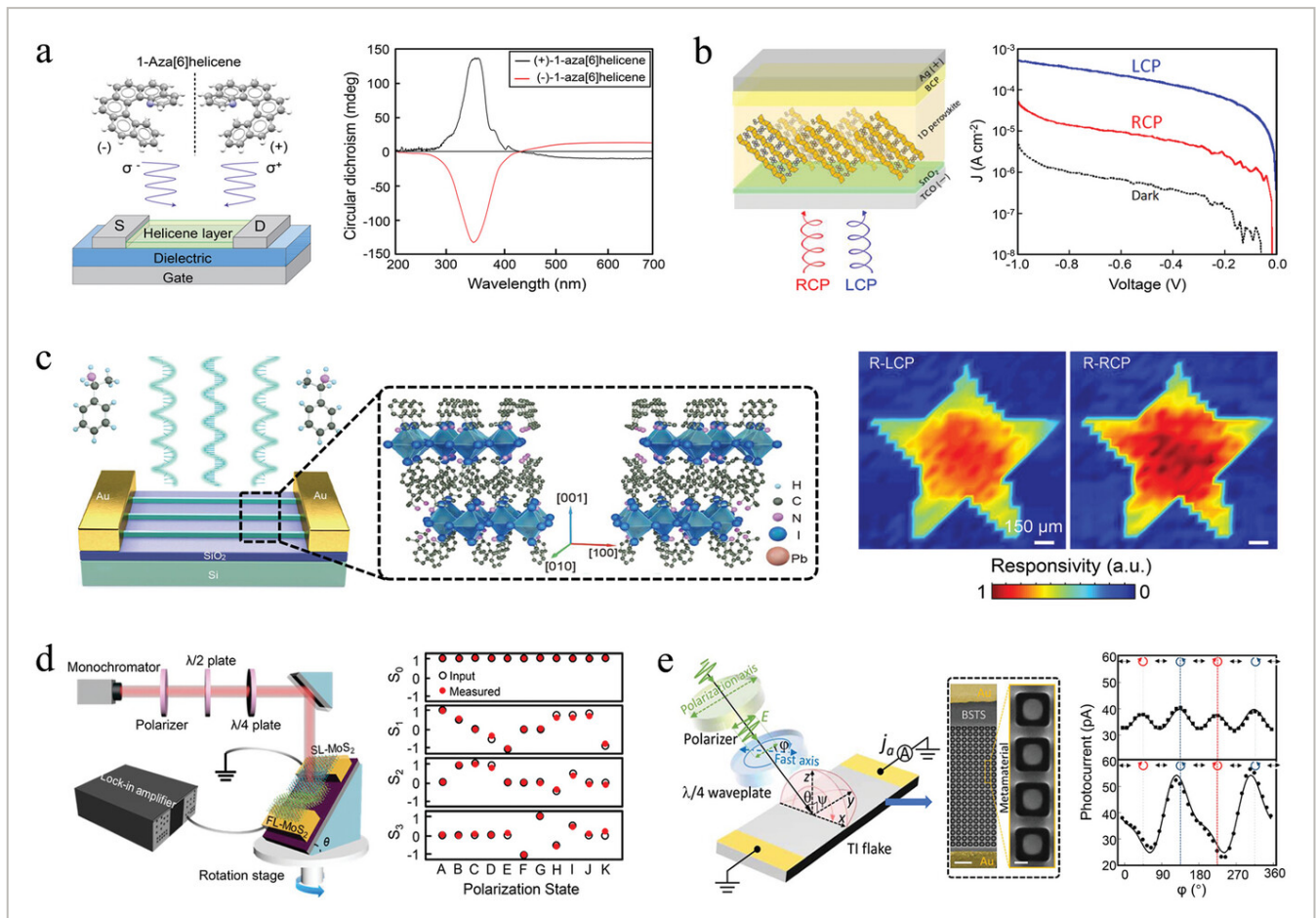


**Figure 7**

[Open in figure viewer](#) | [PowerPoint](#)

Typical LDPPs for circular polarized light detection or full-Stokes polarimetry. a–c) Schematics and circular polarized light-dependent circular dichroism spectra/ photocurrent densities/photocurrent maps of organic semiconductors (1-aza[6]helicene)/1D (NEA)<sub>2</sub>PbI<sub>4</sub> perovskite nanowires whose structures are chiral intrinsically. d) Schematic and input/measured Stokes parameters of the single-layer/few-layer MoS<sub>2</sub> homojunction. e) Schematic, optical image and the enhanced photocurrent of a topological insulator Bi<sub>1.5</sub>Sb<sub>0.5</sub>Te<sub>1.8</sub>Se<sub>1.2</sub> flake. a) Reproduced with permission.<sup>[249]</sup> Copyright 2013, Springer Nature. b) Reproduced with permission.<sup>[251]</sup> Copyright 2020, The Authors, published by American Association for the Advancement of Science. From ref. [251]. Copyright The Authors, some rights reserved; exclusive licensee AAAS. Distributed under a CC BY-NC 4.0 license <http://creativecommons.org/licenses/by-nc/4.0/>. Reprinted with permission from AAAS. c) Reproduced with permission.<sup>[139]</sup> Copyright 2021, American Chemical Society. d) Reproduced with permission.<sup>[259]</sup> Copyright 2021, American Chemical Society. e) Reproduced with permission.<sup>[260]</sup> Copyright 2021, American Association for the Advancement of Science. From ref. [260]. Copyright The Authors, some

Here, we should also emphasize that most of LDPPs mentioned above can only selectively respond to the linear or circular polarized light at present. The simultaneous detection of them is conducive to the full-Stokes polarimetry imaging of targets, which is significant in practice. In order to achieve the goal, people start their work from the perspective of material selection, work model optimization and advantages complement between above different type of devices. In 2021, Wu's group prepared an array of single-crystal nanowires based on the chiral perovskite  $(\text{PEA})_2\text{PbI}_4$  and further designed a Stokes-parameter photodetector.<sup>[139]</sup> The selective attenuation of 1D material arrays on electromagnetic field and the intrinsic polarization-dependent photoconductivity of the chiral material are both considered (Figure 7c). In the same year, Fang et al. carried out another experiment by using a single-layer/few-layer  $\text{MoS}_2$  homojunction.<sup>[259]</sup> Based on the in-plane to out-of-plane optical response to the material under total reflection and the valley-dependent nonequivalent excitation caused by CPGE, four Stokes parameters in the 650–690 nm band were detected efficiently (Figure 7d). In another work, Soci's group combined the spin transport of a TI material ( $\text{Bi}_{1.5}\text{Sb}_{0.5}\text{Te}_{1.8}\text{Se}_{1.2}$ ) with the field regulation of metamaterials to carry out a polarization-dependent research later.<sup>[260]</sup> A 11-fold enhancement of the CPGE and a  $\approx 0.87$  photocurrent dichroism were observed, shown in Figure 7e.

## 4 Outlook and Summary

Despite much progress made on the study of LDPPs, the devices still face plenty of challenges before applications. We will mainly discuss from the view of comprehensive performance enhancement, integrated manufacturing and intelligent applications of devices here. We believe that great opportunities lie ahead of us and can push the field into new space if these issues are addressed effectively (Figure 8a).

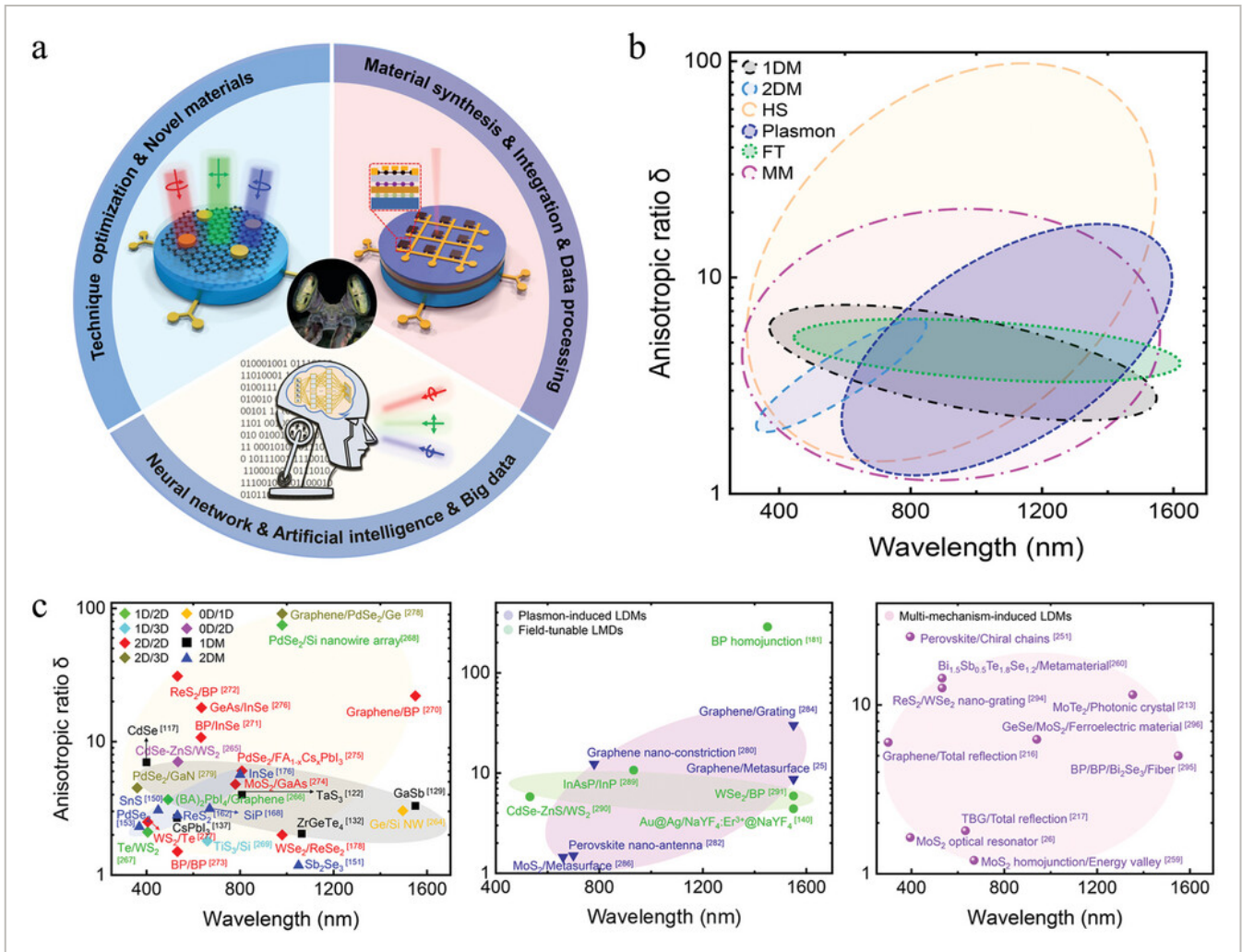


**Figure 8**

[Open in figure viewer](#) | [PowerPoint](#)

a) Opportunities and challenges faced with LDPs in their future development. b,c) Anisotropic ratio against wavelength for the different representative LDPs. The HS, FT and MM are abbreviations for LDM-based heterostructure, field-induced LDMs and multimechanism-induced LDMs, respectively. Since there are relatively few devices working in the ultraviolet and infrared bands at present, the devices concerned here are focused in the range of  $\approx 200$ – $1700$  nm.

## 4.1 Comprehensive Performance Enhancement

For LDM-based photodetectors, the comprehensive performance improvement has always been a problem to be considered. Here, we will leave aside the common issues, such as the low light absorption of LDMs, trade-off between responsivity and response speed, and large dark current especially in the infrared range, that faced in conventional devices and mainly focus on the problems in LDPs. The pros and cons of each type of devices have been described in Sections 7–9, and here we make a brief summary as follows:

The type-I LDPs are usually designed as a simple configuration working under a relatively clear principle. Various photosensitive materials can be chosen from and the response

range covers from ultraviolet to infrared bands. Nevertheless, a single material cannot selectively detect the linear/circular polarized information of a target at the same time, and the anisotropic ratios of the related devices are usually lower than 5, which is not conducive to the high-resolution monitor of polarized information. These drawbacks are mainly due to the intrinsic properties of materials related to their lattice symmetries. How to fundamentally improve the anisotropy of a material will play a crucial role in its practical applications in polarized photodetection. In contrast, the type-II LDPPs can achieve ultrahigh polarized photoresponse due to their flexible device configurations and effective regulation of electromagnetic fields. They are also considered to be the closest to practical applications. However, their developments are usually limited by the demanding preparations. Sometimes we need to spend huge effort to implement certain functions of the device, such as high responsivity and anisotropic ratio at specified band. Compared to them, the type-III LDPPs have the most room for development. By controlling the nonlinear light-matter interactions, the zero-bias full-Stokes polarimetry can be realized in a simple mode. One can even drive some of the materials with photon energies smaller than their energy band gaps due to the multiphoton nonlinear physical processes. However, the weak nonlinear interactions may obliterate the current into the linear photoresponse, which sets up great barriers for the practical applications of such devices. The technical combination between excitation of nonlinear photoresponse and polarized photodetection is also an important issue that needs to be considered.

To compensate for these deficiencies, one can work from the view of the material selection and technology optimization. One hand, the novel LDMs or their composites with excellent intrinsic properties should be explored constantly. For instance, the moiré superlattices whose properties can be tuned by controlling the interlayer rotation angles are likely to provide a breakthrough in device performance.<sup>[27, 261, 262]</sup> On the other hand, the advantages complementarity between different type of LDPPs should also be focused on. As an example mentioned above, the intrinsic advantages of LDMs and related devices can be further amplified with combining their nonlinear photoresponse with local field modulations.<sup>[139, 259, 260]</sup> The device configurations can also be rich and diverse due to the various forms of local fields.<sup>[47]</sup> To avoid repeating the content of other similar articles, here we provide a simple performance comparison of existing devices in **Table 6** and Figure **8b**.<sup>[23, 25, 26, 140, 178, 180, 181, 197, 213, 216, 217, 251, 256, 259, 260, 263-296]</sup>

**Table 6.** Performance regulation of different LDPPs

Heterostructures	0D/1D	CdSe@CdS/PVDF	200–405	–
		Ge/Si NW	1200–1700	5.5@1500

Type		Materials	Response band [nm]	R [A W <sup>-1</sup> m <sup>-2</sup> nm <sup>-1</sup> ]
	0D/2D	CdSe-ZnS/WS <sub>2</sub>	532	≈10 <sup>4</sup>
	1D/2D	(BA) <sub>2</sub> PbI <sub>4</sub> /Graphene	480–600	≈0.3 : 10 <sup>-3</sup> @4 nm
		Te/WS <sub>2</sub>	400–700	27.7@405
		PdSe <sub>2</sub> /Si nanowire array	200–4600	0.726@9 nm
	1D/3D	TiS <sub>3</sub> /Si	405–1050	35 × 10 <sup>-3</sup> @6 nm

- a) The slash here separates the response band from the specific response wavelength of the device;
- b) The “C” represents the device responding to circular polarized light.
- c) The “G” and “F” are abbreviations for “photogating field” and “ferroelectric field”, respectively. Strictly speaking, the built-in field (talked in Heterostructures) and localized electromagnetic field (talked in Plasmon-induced LDMs) should also be included in the field-tunable devices. But because the first two items involve many work, they are listed separately here.

## 4.2 Integrated Manufacturing

During the integrated manufacturing and applications in the future, the LDPPs will generally face the challenges such as high-quality synthesis of materials, processing and integration of micro/nanostructures, as well as the later data extraction and analysis, etc. First, limited by the working modes especially in the DFP-PPs, the applicable materials are still confined to the 1D nanostructure arrays, 2D materials or their heterostructures. This puts forward high requirement for the material preparation, at least needs to ensure the complete crystallinity with fewer defects at a centimeter scale. Meanwhile, the high-quality transfer, topography processing, doping and other operations are also critical for avoiding the device performance degradations subsequently.<sup>[28]</sup> The second challenge need to be considered is the technical compatibility during device integration. Although the silicon semiconductor production technologies can meet most of our requirements, we still need to carry out experiments in terms of the time and economic costs. Finally, we should also pay attention to the data processing, such as signal extraction, calibration, denoising and analysis especially in the brand-new working modes. As an example, the performance of the type-III

LDPPs is closely related to the material symmetry, incident angle and helicity of light.<sup>[78]</sup> The numerous influencing factors make any changes in experiment may lead to a signal deviation. The accurate and efficient data processing is an important step toward the practical application of related devices.<sup>[67-70]</sup>

### 4.3 Intelligent Application

The intelligent application of LDPPs is an inevitable direction for the development. We can imagine that the PP with high performance, integration and multifunction can become one of the most important source components in the digital terminal equipment. The detector of the future must be a deep optical sensing device that can monitor multidimensional information, including the light intensity, wavelength, polarization, phase and even angular momentum.<sup>[297]</sup> Meanwhile, the information obtained from PPs can be involved in big data storage and analyzed by artificial intelligence, which can further guide the functional applications of the PPs in reverse (Figure 8a). Nevertheless, the road is certainly full of challenges. The performance improvement of the PP itself, massive information handling and efficient man–machine interaction, etc. are all issues need to be paid attention to. While considering the effective integration of multiple technologies, innovative sensing materials and new physical mechanisms are also need to be explored constantly. It is believed that these problems will be addressed finally through the joint efforts of various related fields.

In conclusion, the developments of LDPPs made of the 1D nanowires/tubes/arrays, 2D materials and their heterostructures are mainly introduced in this review. The working principle and response mechanisms of related devices are also discussed. Significantly, the existing LDPPs are creatively divided into three categories from the perspective of constitutive equation, and the representative works of each type are presented. Finally, we discuss the challenges and opportunities in this area. Compared with the traditional photodetectors, the LDPPs as emergent devices have more room for development. They are perfect complements to traditional devices, and even can be substitute candidates in some special fields. With the advent of the post-Moore era, we believe that the LDPPs will be widely concerned and can play an increasingly important role in the future.

## Acknowledgements

This work was supported by the National Key Research and Development Program of China (Grant No. 2023YFB3611400), the National Natural Science Foundation of China (12274065, 52025022, 62250065, 12004069, 52002056), the Foundation of Jilin Educational Committee (JJKH20221151KJ), the Open Fund of State Key Laboratory of Infrared Physics (SITP-NLIST-YB-2023-11), the Fundamental Research Funds for the Central Universities (2412021QD004, 2412021ZD006), and the International Partnership Program of Chinese Academy of Sciences (181331KYSB20200012).



## Conflict of Interest

The authors declare no conflict of interest.

## Biographies



**Wei Xin** received his B.S. degree from the Changchun University of Science and Technology and Ph.D. degree from Nankai University. He then continued his research in the Changchun Institute of Optics, Fine Mechanics and Physics, Chinese Academy of Sciences (CAS), Zhejiang University and Shanghai Institute of Technical Physics, CAS, respectively. He is currently an associate professor in the Key Laboratory of UV-Emitting Materials and Technology, Ministry of Education, Northeast Normal University. His research focuses on the 2D-material-based micro/nano-optoelectronic devices.



**JinLuo Cheng** received the graduate degree with majors in applied physics and the Ph.D. degree in condensed matter physics, both from the University of Science and Technology of China, Hefei, China, in 2002 and 2007, respectively. He is currently a professor at the Changchun Institute of Optics, Fine Mechanics and Physics, Chinese Academy of Sciences (CAS), China. He has coauthored 60 peer-reviewed journal papers. His current research interests focus on the nonlinear optics and light matter interaction in 2D materials.



**Weida Hu** received his Ph.D. degree (with honors) in microelectronics and solid-state electronics from the Shanghai Institute of Technology Physics (SITP), Chinese Academy of Sciences (CAS), in 2007. He is currently a full professor (Principal investigator) on fabrication and characterization of infrared photodetectors/photodiodes/phototransistors and their smart chips in SITP, CAS. He received the National Science Fund for Distinguished Young Scholars in 2017. He has authored or coauthored more than 200 technical journal papers and conference presentations with the total citations of 16 000 and an *h*-index of 70 (Google Scholar).



**Haiyang Xu** received his Ph.D. degree from the Changchun Institute of Optics, Fine Mechanics and Physics, Chinese Academy of Sciences in 2006. During 2006–2008, he worked as a postdoctoral fellow in the Chinese University of Hong Kong. Currently, he is a professor at the Key Laboratory of UV-Emitting Materials and Technology, Ministry of Education, Northeast Normal University. His research interests include wide-bandgap semiconductor materials and their photonic/electronic devices, memristive materials and devices, and artificial synaptics.

## References



1 G. Wang, R. Wang, W. Kong, J. Zhang, *Cogn. Neurodynamics* 2018, 12, 615.

[PubMed](#) | [Web of Science®](#) | [Google Scholar](#) | [Find It @ Hanyang](#)

2 V. Ronchi, V. Barocas, *The Nature of Light: An Historical Survey*, Harvard University Press, Cambridge, MA, USA 1970.

[Google Scholar](#) | [Find It @ Hanyang](#)

---

3 S. Huard, *Polarization of Light*, Wiley, Hoboken, NJ, USA 1997.

[Google Scholar](#) | [Find It @ Hanyang](#)

---

4 B. L. Barge, *J. Rech. Atmos.* 1974, **8**, 163.

[Google Scholar](#) | [Find It @ Hanyang](#)

---

5 G. C. McCormick, A. Hendry, *Radio Sci.* 1975, **10**, 421.

[Web of Science®](#) | [Google Scholar](#) | [Find It @ Hanyang](#)

---

6 M. F. Sterzik, S. Bagnulo, E. Palle, *Nature* 2012, **483**, 64.

[CAS](#) | [PubMed](#) | [Web of Science®](#) | [Google Scholar](#) | [Find It @ Hanyang](#)

---

7 S. B. Powell, R. Garnett, J. Marshall, C. Rizk, V. Gruev, *Sci. Adv.* 2018, **4**, eaao6841.

[PubMed](#) | [Web of Science®](#) | [Google Scholar](#) | [Find It @ Hanyang](#)

---

8 X. Li, Z. Sun, S. Lu, K. Omasa, *Remote Sens. Environ.* 2021, **253**, 112230.

[Google Scholar](#) | [Find It @ Hanyang](#)

---

9 D. M. Jameson, J. A. Ross, *Chem. Rev.* 2010, **110**, 2685.

[CAS](#) | [PubMed](#) | [Web of Science®](#) | [Google Scholar](#) | [Find It @ Hanyang](#)

---

10 T. A. Seliga, V. N. Bringi, *J. Appl. Meteorol. Clim.* 1976, **15**, 69.

[Google Scholar](#) | [Find It @ Hanyang](#)

---

11 F. M. Bréon, P. Y. Deschamps, *Remote Sens. Environ.* 1993, **43**, 193.

[Web of Science®](#) | [Google Scholar](#) | [Find It @ Hanyang](#)

---

12 N. Gupta, *Proc. SPIE* 2002, **4574**, 184.

[Google Scholar](#) | [Find It @ Hanyang](#)

---

13 A. M. Phenis, M. Virgen, E. E. de Leon, *Proc. SPIE* 2005, **5875**, 587502.

[Google Scholar](#) | [Find It @ Hanyang](#)

---

14 S. Moultrie, M. Roche, A. Lompadro, D. Chenault, *Proc. SPIE* 2007, **6682**, 66820B.

[Google Scholar](#) | [Find It @ Hanyang](#)

---

15 N. R. Malone, A. Kennedy, R. Graham, Y. Thai, J. Stark, J. Sienicki, E. Fest, *Proc. SPIE* 2011, **8154**, 81540T.

[Google Scholar](#) | [Find It @ Hanyang](#)

---

16 J. Craven-Jones, M. Kudenov, M. Stapelbroek, E. Dereniak, *Appl. Optics* 2011, **50**, 1170.

[PubMed](#) | [Web of Science®](#) | [Google Scholar](#) | [Find It @ Hanyang](#)

---

17 J. Qi, C. He, D. S. Elson, *Biomed. Opt. Express* 2017, **8**, 4933.

[CAS](#) | [PubMed](#) | [Web of Science®](#) | [Google Scholar](#) | [Find It @ Hanyang](#)

---

18 B. M. Ratliff, G. C. Sargent, *Proc. SPIE* 2022, **12112**, 1211206.

[Google Scholar](#) | [Find It @ Hanyang](#)

---

19 J. Wang, M. S. Gudixsen, X. Duan, Y. Cui, C. M. Lieber, *Science* 2001, **293**, 1455.

[CAS](#) | [PubMed](#) | [Web of Science®](#) | [Google Scholar](#) | [Find It @ Hanyang](#)

---

20 T. J. Echtermeyer, L. Britnell, P. K. Jasnós, A. Lombardo, R. V. Gorbachev, A. N. Grigorenko, A. K. Geim, A. C. Ferrari, K. S. Novoselov, *Nat. Commun.* 2011, **2**, 458.

[CAS](#) | [PubMed](#) | [Web of Science®](#) | [Google Scholar](#) | [Find It @ Hanyang](#)

---

21 J. W. Mclver, D. Hsieh, H. Steinberg, P. Jarillo-Herrero, N. Gedik, *Nat. Nanotechnol.* 2012, **7**, 96.

[CAS](#) | [Web of Science®](#) | [Google Scholar](#) | [Find It @ Hanyang](#)

---

22 H. Yuan, X. Liu, F. Afshinmanesh, W. Li, G. Xu, J. Sun, B. Lian, A. G. Curto, G. Ye, Y. Hikita, Z. Shen, S. Zhang, X. Chen, M. Brongersma, H. Y. Hwang, Y. Cui, *Nat. Nanotechnol.* 2015, **10**, 707.

[CAS](#) | [PubMed](#) | [Web of Science®](#) | [Google Scholar](#) | [Find It @ Hanyang](#)

---

23 L. Tong, X. Duan, L. Song, T. Liu, L. Ye, X. Huang, P. Wang, Y. Sun, X. He, L. Zhang, K. Xu, W. Hu, J. Xu, J. Zang, G. J. Cheng, *Appl. Mater. Today* 2019, **15**, 203.

[Web of Science®](#) | [Google Scholar](#) | [Find It @ Hanyang](#)

---

24 T. Zou, B. Zhao, W. Xin, Y. Wang, B. Wang, X. Zheng, H. Xie, Z. Zhang, J. Yang, C. Guo, *Light: Sci. Appl.* 2020, **9**, 69.

[CAS](#) | [PubMed](#) | [Web of Science®](#) | [Google Scholar](#) | [Find It @ Hanyang](#)

---

25 L. Li, J. Wang, L. Kang, W. Liu, L. Yu, B. Zheng, M. L. Brongersma, D. H. Werner, S. Lan, Y. Shi, X. Wang, *ACS Nano* 2020, **14**, 16634.

[CAS](#) | [PubMed](#) | [Web of Science®](#) | [Google Scholar](#) | [Find It @ Hanyang](#)

---

26 T. Deng, S. Li, Y. Li, Y. Zhang, J. Sun, W. Yin, W. Wu, M. Zhu, Y. Wang, Z. Liu, *Nanophotonics* 2020, **9**, 4719.

[CAS](#) | [Web of Science®](#) | [Google Scholar](#) | [Find It @ Hanyang](#)

---

27 C. Ma, S. Yuan, P. Cheung, K. Watanabe, T. Taniguchi, F. Zhang, F. Xia, *Nature* 2022, **604**, 266.

[CAS](#) | [PubMed](#) | [Web of Science®](#) | [Google Scholar](#) | [Find It @ Hanyang](#)

---

28 C. Chang, W. Chen, Y. Chen, Y. Chen, Y. Chen, F. Ding, C. Fan, H. Fan, Z. Fan, C. Gong, Y. Gong, Q. He, X. Hong, S. Hu, W. Hu, W. Huang, Y. Huang, W. Ji, D. Li, L. Li, Q. Li, L. Lin, C. Ling, M. Liu, N. Liu, Z. Liu, K. P. Loh, J. Ma, F. Miao, H. Peng, *Acta Phys. Chim. Sin.* 2022, **37**, 2108017.

[Google Scholar](#) | [Find It @ Hanyang](#)

---

29 Z. Xie, B. Zhang, Y. Ge, Y. Zhu, G. Nie, Y. Song, C. K. Lim, H. Zhang, P. N. Prasad, *Chem. Rev.* 2022, **122**, 1127.

[CAS](#) | [PubMed](#) | [Web of Science®](#) | [Google Scholar](#) | [Find It @ Hanyang](#)

---

30 M. Chen, L. Li, M. Xu, W. Li, L. Zheng, X. Wang, *Research* 2023, **6**, 0066.

[CAS](#) | [PubMed](#) | [Google Scholar](#) | [Find It @ Hanyang](#)

---

31 R. Kumar, E. Joanni, S. Sahoo, J. Shim, W. Tan, A. Matsuda, R. K. Singh, *Carbon* 2022, **193**, 298.

[CAS](#) | [Web of Science®](#) | [Google Scholar](#) | [Find It @ Hanyang](#)

---

32 F. P. G. De Arquer, D. V. Talapin, V. I. Klimov, Y. Arakawa, M. Bayer, E. H. Sargent, *Science* 2021, **373**, eaaz8541.

[PubMed](#) | [Web of Science®](#) | [Google Scholar](#) | [Find It @ Hanyang](#)

---

33 R. Xiang, T. Inoue, Y. Zheng, A. Kumamoto, Y. Qian, Y. Sato, M. Liu, D. Tang, D. Gokhale, J. Guo, K. Hisama, S. Yotsumoto, T. Ogamoto, H. Arai, Y. Kobayashi, H. Zhang, B. Hou, A. Anisimov, M. Maruyama, Y. Miyata, S. Okada, S. Chiashi, Y. Li, J. Kong, E. I. Kauppinen, Y. Ikuhara, K. Suenaga, S. Maruyama, *Science* 2020, **367**, 537.

[CAS](#) | [PubMed](#) | [Web of Science®](#) | [Google Scholar](#) | [Find It @ Hanyang](#)

---

34 K. Deng, Z. Luo, L. Tan, Z. Quan, *Chem. Soc. Rev.* 2020, **49**, 6002.

[CAS](#) | [Web of Science®](#) | [Google Scholar](#) | [Find It @ Hanyang](#)

---

35 Q. Zhang, E. Li, Y. Wang, C. Gao, C. Wang, L. Li, D. Geng, H. Chen, W. Chen, W. Hu, *Adv. Mater.* 2023, **35**, 2208600.

[CAS](#) | [Web of Science®](#) | [Google Scholar](#) | [Find It @ Hanyang](#)

---

36 G. Hu, *Nature* 2020, **582**, 209.

[CAS](#) | [PubMed](#) | [Web of Science®](#) | [Google Scholar](#) | [Find It @ Hanyang](#)

---

37 X. Gao, X. Li, W. Xin, X. Chen, Z. Liu, J. Tian, *Nanophotonics* 2020, **9**, 1717.

[CAS](#) | [Web of Science®](#) | [Google Scholar](#) | [Find It @ Hanyang](#)

---

38 H. Zhou, C. Sun, W. Xin, Y. Li, Y. Chen, H. Zhu, *Nano Lett.* 2022, **22**, 2547.

[CAS](#) | [PubMed](#) | [Web of Science®](#) | [Google Scholar](#) | [Find It @ Hanyang](#)

---

39 Y. Chen, Y. Li, Y. Zhao, H. Zhou, H. Zhu, *Sci. Adv.* 2019, **5**, eaax9958.

[CAS](#) | [PubMed](#) | [Web of Science®](#) | [Google Scholar](#) | [Find It @ Hanyang](#)

---

40 R. R. LaPierre, M. Robson, K. M. Azizur-Rahman, P. Kuyanov, *J. Phys. Appl. Phys.* 2017, **50**, 123001.

[Web of Science®](#) | [Google Scholar](#) | [Find It @ Hanyang](#)

---

41 X. Liu, Q. Guo, J. Qiu, *Adv. Mater.* 2017, **29**, 1605886.

[CAS](#) | [Web of Science®](#) | [Google Scholar](#) | [Find It @ Hanyang](#)

---

42 A. D. Yoffe, *Adv. Phys.* 2002, **51**, 799.

[Web of Science®](#) | [Google Scholar](#) | [Find It @ Hanyang](#)

---

43 N. Barnes, *Nat. Rev. Methods Primers* 2023, **2**, 57.

[Google Scholar](#) | [Find It @ Hanyang](#)

---

44 Y. Li, T. Zhuang, Y. Lin, J. Tian, X. Qi, X. Li, R. Wang, L. Wu, G. Liu, T. Ma, Z. He, H. Sun, F. Fan, H. Zhu, S. Yu, *J. Am. Chem. Soc.* 2021, **143**, 7013.

[CAS](#) | [PubMed](#) | [Web of Science®](#) | [Google Scholar](#) | [Find It @ Hanyang](#)

---

45 J. Qin, C. Wang, L. Zhen, L. Li, C. Xu, Y. Chai, *Prog. Mater. Sci.* 2021, **122**, 100856.

[CAS](#) | [Web of Science®](#) | [Google Scholar](#) | [Find It @ Hanyang](#)

---

46 J. Wang, H. Fang, X. Wang, X. Chen, W. Lu, W. Hu, *Small* 2017, **13**, 1700894.

[CAS](#) | [Web of Science®](#) | [Google Scholar](#) | [Find It @ Hanyang](#)

---

47 W. Lian, C. Jiang, Y. Yin, R. Tang, G. Li, L. Zhang, B. Che, T. Chen, *Nat. Commun.* 2021, **12**, 3260.

[CAS](#) | [PubMed](#) | [Web of Science®](#) | [Google Scholar](#) | [Find It @ Hanyang](#)

---

48 T. Bai, B. Yang, J. Chen, D. Zheng, Z. Tang, X. Wang, Y. Zhao, R. Lu, K. Han, *Adv. Mater.* 2021, **33**, 2007215.

[CAS](#) | [Web of Science®](#) | [Google Scholar](#) | [Find It @ Hanyang](#)

---

49 Y. Chen, Y. Wang, Z. Wang, Y. Gu, Y. Ye, X. Chai, J. Ye, Y. Chen, R. Xie, Y. Zhou, Z. Hu, Q. Li, L. Zhang, F. Wang, P. Wang, J. Miao, J. Wang, X. Chen, W. Lu, P. Zhou, W. Hu, *Nat. Electron.* 2021, **4**, 357.

[CAS](#) | [Web of Science®](#) | [Google Scholar](#) | [Find It @ Hanyang](#)

---

50 X. Yu, P. Yu, D. Wu, B. Singh, Q. Zeng, H. Lin, W. Zhou, J. Lin, K. Suenaga, Z. Liu, Q. Wang, *Nat. Commun.* 2018, **9**, 1545.

[PubMed](#) | [Web of Science®](#) | [Google Scholar](#) | [Find It @ Hanyang](#)

---

51 Q. Bai, X. Huang, Y. Guo, S. Du, C. Sun, L. Hu, R. Zheng, Y. Yang, A. Jin, J. Li, C. Gu, *Nano Res.* 2023, **16**, 10272.

[CAS](#) | [Web of Science®](#) | [Google Scholar](#) | [Find It @ Hanyang](#)

---

52 G. Li, S. Wang, X. Chen, W. Lu, *Appl. Phys. Lett.* 2014, **104**, 231104.

[Web of Science®](#) | [Google Scholar](#) | [Find It @ Hanyang](#)

---

53 Y. R. Shen, *The Principles of Nonlinear Optics*, Wiley, Hoboken, NJ, USA 1984.

[Google Scholar](#) | [Find It @ Hanyang](#)

---

54 M. Born, E. Wolf, *Principles of Optics: Electromagnetic Theory of Propagation, Interference and Diffraction of Light*, Cambridge University Press, Cambridge, UK 1999.

[Google Scholar](#) | [Find It @ Hanyang](#)

---

55 J. Cheng, J. Sipe, S. Wu, C. Guo, *APL Photonics* 2019, **4**, 034201.

[Google Scholar](#) | [Find It @ Hanyang](#)

---

56 C. He, H. He, J. Chang, B. Chen, H. Ma, M. J. Booth, *Light: Sci. Appl.* 2021, **10**, 194.

[CAS](#) | [PubMed](#) | [Web of Science®](#) | [Google Scholar](#) | [Find It @ Hanyang](#)

---

57 B. Laude-Boulesteix, A. De Martino, B. Drevillon, L. Schwartz, *Appl. Opt.* 2004, **43**, 2824.

[PubMed](#) | [Web of Science®](#) | [Google Scholar](#) | [Find It @ Hanyang](#)

---

58 S. Alali, A. Gribble, I. A. Vitkin, *Opt. Lett.* 2016, **41**, 1038.



[PubMed](#) | [Web of Science®](#) | [Google Scholar](#) | [Find It @ Hanyang](#)

---

59 E. Compain, B. Drevillon, *Appl. Opt.* 1998, **37**, 5938.

[CAS](#) | [PubMed](#) | [Web of Science®](#) | [Google Scholar](#) | [Find It @ Hanyang](#)

---

60 A. Peinado, A. Turpin, A. Lizana, E. Fernández, J. Mompert, J. Campos, *Opt. Lett.* 2013, **38**, 4100.

[PubMed](#) | [Web of Science®](#) | [Google Scholar](#) | [Find It @ Hanyang](#)

---

61 A. Lqbal, M. G. Garcia, L. Chellappan, N. Gans, *Proc. SPIE* 2022, **31**, 033041.

[Google Scholar](#) | [Find It @ Hanyang](#)

---

62 T. M. Cronin, N. Justin Marshall, *Nature* 1989, **339**, 137.

[Web of Science®](#) | [Google Scholar](#) | [Find It @ Hanyang](#)

---

63 I. M. Daly, M. J. How, J. C. Partridge, S. E. Temple, N. J. Marshall, T. W. Cronin, N. W. Roberts, *Nat. Commun.* 2016, **7**, 12140.

[CAS](#) | [PubMed](#) | [Web of Science®](#) | [Google Scholar](#) | [Find It @ Hanyang](#)

---

64 M. Garcia, T. Davis, S. Blair, N. Cui, V. Gruev, *Optica* 2018, **5**, 1240.

[CAS](#) | [Web of Science®](#) | [Google Scholar](#) | [Find It @ Hanyang](#)

---

65 M. Garcia, C. Edmiston, R. Marinov, A. Vail, V. Gruev, *Optica* 2017, **4**, 1263.

[CAS](#) | [Web of Science®](#) | [Google Scholar](#) | [Find It @ Hanyang](#)

---

66 N. A. Rubin, G. D'Aversa, P. Chevalier, Z. Shi, W. Chen, F. Capasso, *Science* 2019, **365**, eaax1839.

[CAS](#) | [PubMed](#) | [Web of Science®](#) | [Google Scholar](#) | [Find It @ Hanyang](#)

---

67 R. M. A. Azzam, *J. Opt. Soc. Am. A* 2016, **33**, 1396.

[CAS](#) | [Google Scholar](#) | [Find It @ Hanyang](#)

---

68 O. Arteaga, J. Freudenthal, B. Wang, B. Kahr, *Appl. Opt.* 2012, **51**, 6805.

[PubMed](#) | [Web of Science®](#) | [Google Scholar](#) | [Find It @ Hanyang](#)

---

69 J. S. Tyo, *Appl. Opt.* 2002, **41**, 619.

[PubMed](#) | [Web of Science®](#) | [Google Scholar](#) | [Find It @ Hanyang](#)

---

70 D. H. Goldstein, R. A. Chipman, *J. Opt. Soc. Am. A* 1990, **7**, 693.

[CAS](#) | [Google Scholar](#) | [Find It @ Hanyang](#)

---

71 M. Buscema, J. O. Island, D. J. Groenendijk, S. I. Blanter, G. A. Steele, H. S. J. van der Zant, A. Castellanos-Gomez, *Chem. Soc. Rev.* 2015, **44**, 3691.

[CAS](#) | [PubMed](#) | [Web of Science®](#) | [Google Scholar](#) | [Find It @ Hanyang](#)

---

72 C. Soci, A. Zhang, X. Bao, H. Kim, Y. Lo, D. Wang, *J. Nanosci. Nanotechnol.* 2010, **10**, 1430.

[CAS](#) | [PubMed](#) | [Web of Science®](#) | [Google Scholar](#) | [Find It @ Hanyang](#)

---

73 R. Bube, *Photoelectronic Properties of Semiconductors*, Cambridge University Press, Cambridge, UK 1992.

[Google Scholar](#) | [Find It @ Hanyang](#)

---

74 A. Rogalski, *Infrared Detectors*, CRC Press, London, UK 2000.

[Google Scholar](#) | [Find It @ Hanyang](#)

---

75 J. P. Heremans, V. Jovovic, E. S. Toberer, A. Saramat, K. Kurosaki, A. Charoenphakdee, S. Yamanaka, G. J. Snyder, *Science* 2008, **321**, 554.

[CAS](#) | [PubMed](#) | [Web of Science®](#) | [Google Scholar](#) | [Find It @ Hanyang](#)

---

76 C. Liu, Y. Chang, S. Lee, Y. Zhang, Y. Zhang, T. B. Norris, Z. Zhong, *Nano. Lett.* 2015, **15**, 4234.

[CAS](#) | [PubMed](#) | [Web of Science®](#) | [Google Scholar](#) | [Find It @ Hanyang](#)

---

77 C. Bao, P. Zhang, D. Sun, S. Zhou, *Nat. Rev. Phys.* 2022, **4**, 33.

[Google Scholar](#) | [Find It @ Hanyang](#)

---

78 M. M. Glazov, S. D. Ganichev, *Phys. Rep.* 2014, **535**, 101.

[CAS](#) | [Web of Science®](#) | [Google Scholar](#) | [Find It @ Hanyang](#)

---

79 A. Zenkevich, Y. Matveyev, K. Maksimova, R. Gaynutdinov, A. Tolstikhina, V. Fridkin, *Phys. Rev. B* 2014, **90**, 161409.

[CAS](#) | [Web of Science®](#) | [Google Scholar](#) | [Find It @ Hanyang](#)

---

80 J. Liu, F. Xia, F. J. Garcia de Abajo, *Nat. Mater.* 2020, **19**, 830.

[CAS](#) | [PubMed](#) | [Web of Science®](#) | [Google Scholar](#) | [Find It @ Hanyang](#)

---

81 J. L. Cheng, N. Vermeulen, J. E. Sipe, *Sci. Rep.* 2017, **7**, 43843.

[CAS](#) | [PubMed](#) | [Web of Science®](#) | [Google Scholar](#) | [Find It @ Hanyang](#)

---

82 C. Jiang, V. A. Shalygin, V. Y. Panevin, S. N. Danilov, M. M. Glazov, R. Yakimova, S. Lara-Avila, S. Kubatkin, S. D. Ganichev, *Phys. Rev. B* 2011, **84**, 125429.

[CAS](#) | [Web of Science®](#) | [Google Scholar](#) | [Find It @ Hanyang](#)

---

83 H. Fang, W. Hu, *Adv. Sci.* 2017, **4**, 1700323.

[Google Scholar](#) | [Find It @ Hanyang](#)

---

84 V. Augelli, R. Murri, M. Nowak, *Phys. Rev. B* 1989, **39**, 8336.

[CAS](#) | [Web of Science®](#) | [Google Scholar](#) | [Find It @ Hanyang](#)

---

85 H. S. Lee, H. Okada, A. Wakahara, A. Yoshida, T. Ohshima, H. Itoh, *J. Appl. Phys.* 2003, **94**, 276.

[CAS](#) | [Web of Science®](#) | [Google Scholar](#) | [Find It @ Hanyang](#)

---

86 A. V. Galeeva, D. A. Belov, A. S. Kazakov, A. V. Ikonnikov, A. I. Artamkin, L. I. Ryabova, V. V. Volobuev, G. Springholz, S. N. Danilov, D. R. Khokhlov, *Nanomaterials* 2021, **11**, 3207.

[CAS](#) | [PubMed](#) | [Google Scholar](#) | [Find It @ Hanyang](#)

---

87 R. D. Tikhonov, *Solid State Electron.* 2011, **54**, 1625.

[Web of Science®](#) | [Google Scholar](#) | [Find It @ Hanyang](#)

---

88 V. N. Sokolov, V. A. Kochelap, K. W. Kim, *Appl. Phys. Lett.* 2010, **97**, 112112.

[Google Scholar](#) | [Find It @ Hanyang](#)

---

89 A. Carvalho, M. Wang, X. Zhu, A. S. Rodin, H. Su, A. H. Castro Neto, *Nat. Rev. Mater.* 2016, **1**, 16061.

[CAS](#) | [Web of Science®](#) | [Google Scholar](#) | [Find It @ Hanyang](#)

---

90 X. Wang, S. Lan, *Adv. Opt. Photonics* 2016, **8**, 618.

[PubMed](#) | [Web of Science®](#) | [Google Scholar](#) | [Find It @ Hanyang](#)

---

91 J. Feng, X. Yan, Y. Liu, H. Gao, Y. Wu, B. Su, L. Jiang, *Adv. Mater.* 2017, **29**, 1605993.

[CAS](#) | [Web of Science®](#) | [Google Scholar](#) | [Find It @ Hanyang](#)

---

92 M. Long, P. Wang, H. Fang, W. Hu, *Adv. Funct. Mater.* 2019, **29**, 1803807.

[Web of Science®](#) | [Google Scholar](#) | [Find It @ Hanyang](#)

---

93 Y. Chen, C. Sun, H. Zhou, J. Li, W. Xin, H. Xu, H. Zhu, *J. Phys. Chem. Lett.* 2021, **12**, 9989.

[CAS](#) | [PubMed](#) | [Web of Science®](#) | [Google Scholar](#) | [Find It @ Hanyang](#)

---

94 Y. Yao, R. Shankar, P. Rauter, Y. Song, J. Kong, M. Loncar, F. Capasso, *Nano Lett.* 2014, **14**, 3749.

[CAS](#) | [PubMed](#) | [Web of Science®](#) | [Google Scholar](#) | [Find It @ Hanyang](#)

---

95 F. Wang, T. Zhang, R. Xie, Z. Wang, W. Hu, *Nat. Commun.* 2023, **14**, 2224.

[CAS](#) | [PubMed](#) | [Google Scholar](#) | [Find It @ Hanyang](#)

---

96 L. Li, W. Han, L. Pi, P. Niu, J. Han, C. Wang, B. Su, H. Li, J. Xiong, Y. Bando, T. Zhai, *InfoMat* 2019, **1**, 54.

[CAS](#) | [Google Scholar](#) | [Find It @ Hanyang](#)

---

97 X. Li, H. Liu, C. Ke, W. Tang, M. Liu, F. Huang, Y. Wu, Z. Wu, J. Kang, *Laser Photonics Rev.* 2021, **15**, 2100322.

[Web of Science®](#) | [Google Scholar](#) | [Find It @ Hanyang](#)

---

98 Z. Li, B. Xu, D. Liang, A. Pan, *Research* 2020, **2020**, 5464258.

[CAS](#) | [PubMed](#) | [Google Scholar](#) | [Find It @ Hanyang](#)

---

99 X. Wang, A. M. Jones, K. L. Seyler, V. Tran, Y. Jia, H. Zhao, H. Wang, L. Yang, X. Xu, F. Xia, *Nat. Nanotechnol.* 2015, **10**, 517.

[CAS](#) | [PubMed](#) | [Web of Science®](#) | [Google Scholar](#) | [Find It @ Hanyang](#)

---

100 T. Low, R. Roldán, H. Wang, F. Xia, P. Avouris, L. M. Moreno, F. Guinea, *Phys. Rev. Lett.* 2014, **113**, 106802.

[CAS](#) | [PubMed](#) | [Web of Science®](#) | [Google Scholar](#) | [Find It @ Hanyang](#)

---

101 H. Yan, F. Xia, W. Zhu, M. Freitag, C. Dimitrakopoulos, A. A. Bol, G. Tulevski, P. Avouris, *ACS Nano* 2012, **5**, 9854.

[Web of Science®](#) | [Google Scholar](#) | [Find It @ Hanyang](#)

---

102 T. D. Ngo, A. Kashani, G. Imbalzano, K. T. Q. Nguyen, D. Hui, *Compos., Part B: Eng.* 2018, **143**, 172.

[CAS](#) | [Web of Science®](#) | [Google Scholar](#) | [Find It @ Hanyang](#)

---

103 K. Kuroda, J. Reimann, J. Gdde, U. Hfer, *Phys. Rev. Lett.* 2016, **11**, 076801.

[Google Scholar](#) | [Find It @ Hanyang](#)

---

104 Y. H. Chan, D. Y. Qiu, F. H. da Jornada, S. G. Louie, *Proc. Natl. Acad. Sci. USA* 2021, **118**, e1906938118.

[CAS](#) | [PubMed](#) | [Web of Science®](#) | [Google Scholar](#) | [Find It @ Hanyang](#)

---

105 G. Long, R. Sabatini, M. I. Saidaminov, G. Lakhwani, A. Rasmita, X. Liu, E. H. Sargent, W. Gao, *Nat. Rev. Mater.* 2020, **5**, 423.

[Web of Science®](#) | [Google Scholar](#) | [Find It @ Hanyang](#)

---

106 X. Shang, L. Wan, L. Wang, F. Gao, H. Li, *J. Mater. Chem. C* 2021, **10**, 2400.

[Web of Science®](#) | [Google Scholar](#) | [Find It @ Hanyang](#)

---

107 S. V. Zhukovsky, V. E. Babicheva, A. B. Evlyukhin, I. E. Protsenko, A. V. Lavrinenko, A. V. Uskov, *Phys. Rev. X* 2014, **4**, 031038.

[CAS](#) | [Web of Science®](#) | [Google Scholar](#) | [Find It @ Hanyang](#)

---

108 D. Somvanshi, S. Jit, *Mat. Sci. Semicon. Proc.* 2023, **164**, 107598.

[CAS](#) | [Google Scholar](#) | [Find It @ Hanyang](#)

---

109 G. Konstantatos, M. Badioli, L. Gaudreau, J. Osmond, M. Bernechea, F. P. G. de Arquer, F. Gatti, F. H. Koppens, *Nat. Nanotechnol.* 2012, **7**, 363.

[CAS](#) | [PubMed](#) | [Web of Science®](#) | [Google Scholar](#) | [Find It @ Hanyang](#)

---

110 J. Feng, Y. Li, J. Li, Q. Feng, W. Xin, W. Liu, H. Xu, Y. Liu, *Nano Lett.* 2022, **22**, 3699.

[CAS](#) | [PubMed](#) | [Web of Science®](#) | [Google Scholar](#) | [Find It @ Hanyang](#)

---

111 Y. Wang, X. Deng, G. Zhang, J. Wei, J. Zhu, Z. Chen, Z. Zhao, J. Sun, *Opt. Express* 2015, **23**, 13348.

[CAS](#) | [PubMed](#) | [Web of Science®](#) | [Google Scholar](#) | [Find It @ Hanyang](#)

---

112 X. Cai, S. Wang, L. Peng, *Nano Res. Energy* 2023, **2**, e9120058.

[Google Scholar](#) | [Find It @ Hanyang](#)

---

113 S. Park, S. W. Heo, W. Lee, D. Inoue, Z. Jiang, K. Yu, H. Jinno, D. Hashizume, M. Sekino, T. Yokota, K. Fukuda, K. Tajima, T. Someya, *Nature* 2018, **561**, 516.

[CAS](#) | [PubMed](#) | [Web of Science®](#) | [Google Scholar](#) | [Find It @ Hanyang](#)

---

114 R. You, Y. Liu, Y. Hao, D. Han, Y. Zhang, Z. You, *Adv. Mater.* 2019, **32**, 1901981.

[Web of Science®](#) | [Google Scholar](#) | [Find It @ Hanyang](#)

---

115 T. Duan, Y. Xie, W. Xu, X. Wei, J. Cao, *ACS Appl. Electron. Mater.* 2022, **4**, 5602.

[CAS](#) | [Google Scholar](#) | [Find It @ Hanyang](#)

---

116 S. Han, W. Jin, D. Zhang, T. Tang, C. Li, X. Liu, Z. Liu, B. Lei, C. Zhou, *Chem. Phys. Lett.* 2004, **389**, 176.

[CAS](#) | [Web of Science®](#) | [Google Scholar](#) | [Find It @ Hanyang](#)

---

117 A. Singh, X. Li, V. Protasenko, G. Galantai, M. Kuno, H. Xing, D. Jena, *Nano. Lett.* 2007, **7**, 2999.

[CAS](#) | [PubMed](#) | [Web of Science®](#) | [Google Scholar](#) | [Find It @ Hanyang](#)

---

118 Z. Liao, J. Xu, J. Zhang, D. Yu, *Chin. Phys. Lett.* 2008, **25**, 2789.

[Web of Science®](#) | [Google Scholar](#) | [Find It @ Hanyang](#)

---

119 S. N. Dorenbos, E. M. Reiger, N. Akopian, U. Perinetti, V. Zwiller, T. Zijlstra, T. M. Klapwijk, *Appl. Phys. Lett.* 2008, **93**, 161102.

[Web of Science®](#) | [Google Scholar](#) | [Find It @ Hanyang](#)

---

120 L. Cao, J. Park, P. Fan, B. Clemens, M. L. Brongersma, *Nano Lett.* 2010, **10**, 1229.

[CAS](#) | [PubMed](#) | [Web of Science®](#) | [Google Scholar](#) | [Find It @ Hanyang](#)

---

121 Z. Liu, G. Chen, B. Liang, G. Yu, H. Huang, D. Chen, G. Shen, *Opt. Express* 2013, **21**, 7799.

[CAS](#) | [PubMed](#) | [Web of Science®](#) | [Google Scholar](#) | [Find It @ Hanyang](#)

---

122 S. Liu, W. Xiao, M. Zhong, L. Pan, X. Wang, H. Deng, J. Liu, J. Li, Z. Wei, *Nanotechnology* 2018, **29**, 184002.

[PubMed](#) | [Web of Science®](#) | [Google Scholar](#) | [Find It @ Hanyang](#)

---

123 S. Yang, M. Wu, W. Shen, L. Huang, S. Tongay, K. Wu, B. Wei, Y. Qin, Z. Wang, C. Jiang, C. Hu, *ACS Appl. Mater. Interfaces* 2019, **11**, 3342.

[CAS](#) | [PubMed](#) | [Web of Science®](#) | [Google Scholar](#) | [Find It @ Hanyang](#)

---

124 H. Yang, L. Pan, X. Wang, H. Deng, M. Zhong, Z. Zhou, Z. Lou, G. Shen, Z. Wei, *Adv. Funct. Mater.* 2019, **29**, 1904416.

[Web of Science®](#) | [Google Scholar](#) | [Find It @ Hanyang](#)

---

125 Y. Li, Z. Shi, L. Wang, Y. Chen, W. Liang, D. Wu, X. Li, Y. Zhang, C. Shan, X. Fan, *Mater. Horiz.* 2020, 7, 1613.

[CAS](#) | [Web of Science®](#) | [Google Scholar](#) | [Find It @ Hanyang](#)

---

126 M. Luo, F. Ren, N. Gagrani, K. Qiu, Q. Wang, L. Yu, J. Ye, F. Yan, R. Zhang, H. Tan, C. Jagadish, X. Ji, *Adv. Opt. Mater.* 2020, 8, 2000514.

[CAS](#) | [Web of Science®](#) | [Google Scholar](#) | [Find It @ Hanyang](#)

---

127 K. Zhao, J. Yang, M. Zhong, Q. Gao, Y. Wang, X. Wang, W. Shen, C. Hu, K. Wang, G. Shen, M. Li, J. Wang, W. Hu, Z. Wei, *Adv. Funct. Mater.* 2020, 31, 2006601.

[Web of Science®](#) | [Google Scholar](#) | [Find It @ Hanyang](#)

---

128 W. Yang, J. Yang, K. Zhao, Q. Gao, L. Liu, Z. Zhou, S. Hou, X. Wang, G. Shen, X. Pang, Q. Xu, Z. Wei, *Adv. Sci.* 2021, 8, 2100075.

[CAS](#) | [Google Scholar](#) | [Find It @ Hanyang](#)

---

129 Z. Ren, P. Wang, K. Zhang, W. Ran, J. Yang, Y. Liu, Z. Lou, G. Shen, Z. Wei, *IEEE Electron Device Lett.* 2021, 42, 549.

[CAS](#) | [Web of Science®](#) | [Google Scholar](#) | [Find It @ Hanyang](#)

---

130 F. Yang, K. Li, M. Fan, W. Yao, L. Fu, C. Xiong, S. Jiang, D. Li, M. Xu, C. Chen, G. Zhang, J. Tang, *Adv. Opt. Mater.* 2023, 11, 2201859.

[CAS](#) | [Web of Science®](#) | [Google Scholar](#) | [Find It @ Hanyang](#)

---

131 X. Wang, K. Wu, M. Blei, Y. Wang, L. Pan, K. Zhao, C. Shan, M. Lei, Y. Cui, B. Chen, D. Wright, W. Hu, S. Tongay, Z. Wei, *Adv. Electron. Mater.* 2019, 5, 1900419.

[Web of Science®](#) | [Google Scholar](#) | [Find It @ Hanyang](#)

---

132 R. Bai, T. Xiong, J. Zhou, Y. Liu, W. Shen, C. Hu, F. Yan, K. Wang, D. Wei, J. Li, J. Yang, Z. Wei, *Infomat* 2021, 4, e11258.

[Google Scholar](#) | [Find It @ Hanyang](#)



---

133 L. Xiao, Y. Zhang, Y. Wang, K. Liu, Z. Wang, T. Li, Z. Jiang, J. Shi, L. Liu, Q. Li, Y. Zhao, Z. Feng, S. Fan, K. Jiang, *Nanotechnology* 2011, **22**, 025502.

[CAS](#) | [PubMed](#) | [Web of Science®](#) | [Google Scholar](#) | [Find It @ Hanyang](#)

---

134 L. Zhang, Y. Wu, L. Deng, Y. Zhou, C. Liu, S. Fan, *Nano Lett.* 2016, **16**, 6378.

[CAS](#) | [PubMed](#) | [Web of Science®](#) | [Google Scholar](#) | [Find It @ Hanyang](#)

---

135 H. Zhou, J. Wang, C. Ji, X. Liu, J. Han, M. Yang, J. Gou, J. Xu, Y. Jiang, *Carbon* 2019, **143**, 844.

[CAS](#) | [Web of Science®](#) | [Google Scholar](#) | [Find It @ Hanyang](#)

---

136 L. Gao, K. Zeng, J. Guo, C. Ge, J. Du, Y. Zhao, C. Chen, H. Deng, Y. He, H. Song, G. Niu, J. Tang, *Nano Lett.* 2016, **16**, 7446.

[CAS](#) | [PubMed](#) | [Web of Science®](#) | [Google Scholar](#) | [Find It @ Hanyang](#)

---

137 Y. Zhou, J. Luo, Y. Zhao, C. Ge, C. Wang, L. Gao, C. Zhang, M. Hu, G. Niu, J. Tang, *Adv. Opt. Mater.* 2018, **6**, 1800679.

[Web of Science®](#) | [Google Scholar](#) | [Find It @ Hanyang](#)

---

138 X. Sun, W. Zhang, C. Zhang, L. You, G. Xu, J. Huang, H. Zhou, H. Li, Z. Wang, X. Xie, *Opt. Express* 2021, **29**, 11021.

[PubMed](#) | [Web of Science®](#) | [Google Scholar](#) | [Find It @ Hanyang](#)

---

139 Y. Zhao, Y. Qiu, J. Feng, J. Zhao, G. Chen, H. Gao, Y. Zhao, L. Jiang, Y. Wu, *J. Am. Chem. Soc.* 2021, **143**, 8437.

[CAS](#) | [PubMed](#) | [Web of Science®](#) | [Google Scholar](#) | [Find It @ Hanyang](#)

---

140 Y. Ji, G. Fang, J. Shang, X. Dong, J. Wu, X. Lin, W. Xu, B. Dong, *ACS Appl. Mater. Interfaces* 2022, **14**, 50045.

[CAS](#) | [Web of Science®](#) | [Google Scholar](#) | [Find It @ Hanyang](#)

---

141 C. Wu, B. Zeng, K. Zhou, L. Shan, J. Wang, L. Wang, Y. Yang, Y. Zhou, L. Luo, *IEEE Trans. Electron Devices* 2022, **69**, 2469.

[Web of Science®](#) | [Google Scholar](#) | [Find It @ Hanyang](#)

---

---

142 Q. Song, Y. Wang, F. Vogelbacher, Y. Zhan, D. Zhu, Y. Lan, W. Fang, Z. Zhang, L. Jiang, Y. Song, M. Li, *Adv. Energy Mater.* 2021, **11**, 2100742.

[CAS](#) | [Web of Science®](#) | [Google Scholar](#) | [Find It @ Hanyang](#)

---

143 T. Antoni, A. Nedelcu, X. Marcadet, H. Facchetti, V. Berger, *Appl. Phys. Lett.* 2007, **90**, 201107.

[CAS](#) | [Web of Science®](#) | [Google Scholar](#) | [Find It @ Hanyang](#)

---

144 Y. Hou, H. Liang, A. Tang, X. Du, Z. Mei, *Appl. Phys. Lett.* 2021, **118**, 063501.

[CAS](#) | [Google Scholar](#) | [Find It @ Hanyang](#)

---

145 T. Hong, B. Chamlagain, W. Lin, H. Chuang, M. Pan, Z. Zhou, Y. Xu, *Nanoscale* 2014, **6**, 8978.

[CAS](#) | [PubMed](#) | [Web of Science®](#) | [Google Scholar](#) | [Find It @ Hanyang](#)

---

146 J. Qiao, X. Kong, Z. Hu, F. Yang, W. Ji, *Nat. Commun.* 2014, **5**, 4475.

[CAS](#) | [PubMed](#) | [Web of Science®](#) | [Google Scholar](#) | [Find It @ Hanyang](#)

---

147 F. Xia, H. Wang, Y. Jia, *Nat. Commun.* 2014, **5**, 4458.

[CAS](#) | [PubMed](#) | [Web of Science®](#) | [Google Scholar](#) | [Find It @ Hanyang](#)

---

148 J. Qin, H. Xiao, C. Zhu, L. Zhen, C. Xu, *Adv. Opt. Mater.* 2022, **10**, 2195.

[Google Scholar](#) | [Find It @ Hanyang](#)

---

149 P. Li, J. Zhang, C. Zhu, W. Shen, C. Hu, W. Fu, L. Yan, L. Zhou, L. Zheng, H. Lei, Z. Liu, W. Zhao, P. Gao, P. Yu, G. Yang, *Adv. Mater.* 2021, **33**, 2102541.

[CAS](#) | [Web of Science®](#) | [Google Scholar](#) | [Find It @ Hanyang](#)

---

150 Y. Cui, Z. Zhou, X. Wang, X. Wang, Z. Ren, L. Pan, J. Yang, *Nano Res.* 2021, **14**, 2224.

[CAS](#) | [Web of Science®](#) | [Google Scholar](#) | [Find It @ Hanyang](#)

---

151 P. Wan, M. Jiang, L. Su, S. Xia, Y. Wei, T. Xu, Y. Liu, D. Shi, X. Fang, C. Kan, *Adv. Funct. Mater.* 2022, **32**, 2207688.

[CAS](#) | [Web of Science®](#) | [Google Scholar](#) | [Find It @ Hanyang](#)

---

152 X. Wang, Y. Li, L. Huang, X. Jiang, L. Jiang, H. Dong, Z. Wei, J. Li, W. Hu, *J. Am. Chem. Soc.* 2017, **139**, 14976.

[CAS](#) | [PubMed](#) | [Web of Science®](#) | [Google Scholar](#) | [Find It @ Hanyang](#)

---

153 L. Pi, C. Hu, W. Shen, L. Li, P. Luo, X. Hu, P. Chen, D. Li, Z. Li, X. Zhou, T. Zhai, *Adv. Funct. Mater.* 2021, **31**, 2006774.

[CAS](#) | [Web of Science®](#) | [Google Scholar](#) | [Find It @ Hanyang](#)

---

154 J. Qiao, F. Feng, Z. Wang, M. Shen, G. Zhang, X. Yuan, M. G. Somekh, *ACS Appl. Mater. Interfaces* 2021, **13**, 17948.

[CAS](#) | [PubMed](#) | [Web of Science®](#) | [Google Scholar](#) | [Find It @ Hanyang](#)

---

155 Nidhi, S. Das, T. Nautiyal, *ACS Appl. Mater. Interfaces* 2022, **14**, 27444.

[CAS](#) | [Web of Science®](#) | [Google Scholar](#) | [Find It @ Hanyang](#)

---

156 G. Li, H. Zhang, Y. Li, S. Yin, X. Kan, W. Wei, H. Du, B. Ge, C. An, M. Tian, F. Yan, S. Yang, T. Zhai, L. Li, *Nano Res.* 2022, **15**, 5469.

[CAS](#) | [Web of Science®](#) | [Google Scholar](#) | [Find It @ Hanyang](#)

---

157 W. Zhou, J. Chen, H. Gao, T. Hu, S. Ruan, A. Stroppa, W. Ren, *Adv. Mater.* 2019, **31**, 1804629.

[Web of Science®](#) | [Google Scholar](#) | [Find It @ Hanyang](#)

---

158 T. Yang, Y. Li, S. Han, Z. Xu, Y. Liu, X. Zhang, X. Liu, B. Teng, J. Luo, Z. Sun, *Small* 2020, **16**, 1907020.

[CAS](#) | [PubMed](#) | [Web of Science®](#) | [Google Scholar](#) | [Find It @ Hanyang](#)

---

159 L. Li, X. Liu, Y. Li, Z. Xu, Z. Wu, S. Han, K. Tao, M. Hong, J. Luo, Z. Sun, *J. Am. Chem. Soc.* 2019, **141**, 2623.

[CAS](#) | [PubMed](#) | [Web of Science®](#) | [Google Scholar](#) | [Find It @ Hanyang](#)

---

160 M. Li, S. Han, B. Teng, Y. Li, Y. Liu, X. Liu, J. Luo, M. Hong, Z. Sun, *Adv. Opt. Mater.* 2020, **8**, 2000149.

[CAS](#) | [Web of Science®](#) | [Google Scholar](#) | [Find It @ Hanyang](#)

---

161 Y. Liu, Z. Wu, X. Liu, S. Han, Y. Li, T. Yang, Y. Ma, M. Hong, J. Luo, Z. Sun, *Adv. Opt. Mater.* 2019, **7**, 1901049.

[CAS](#) | [Web of Science®](#) | [Google Scholar](#) | [Find It @ Hanyang](#)

---

162 F. Liu, S. Zheng, X. He, A. Chaturvedi, J. He, W. L. Chow, T. R. Mion, X. Wang, J. Zhou, Q. Fu, H. Fan, B. K. Tay, L. Song, R. He, C. Kloc, P. M. Ajayan, Z. Liu, *Adv. Funct. Mater.* 2016, **26**, 1169.

[CAS](#) | [Web of Science®](#) | [Google Scholar](#) | [Find It @ Hanyang](#)

---

163 L. Li, P. Gong, D. Sheng, S. Wang, W. Wang, X. Zhu, X. Shi, F. Wang, W. Han, S. Yang, K. Liu, H. Li, T. Zhai, *Adv. Mater.* 2019, **30**, 1804541.

[Google Scholar](#) | [Find It @ Hanyang](#)

---

164 Y. Wang, P. Wu, Z. Wang, M. Luo, F. Zhong, X. Ge, K. Zhang, M. Peng, Y. Ye, Q. Li, H. Ge, J. Ye, T. He, Y. Chen, T. Xu, C. Yu, Y. Wang, Z. Hu, X. Zhou, C. Shan, M. Long, P. Wang, P. Zhou, W. Hu, *Adv. Mater.* 2010, **32**, 2005037.

[Google Scholar](#) | [Find It @ Hanyang](#)

---

165 X. Chen, W. Mu, Y. Xu, B. Fu, Z. Jia, F. Ren, S. Gu, R. Zhang, Y. Zheng, X. Tao, J. Ye, *ACS Appl. Mater. Interfaces* 2019, **11**, 7131.

[CAS](#) | [PubMed](#) | [Web of Science®](#) | [Google Scholar](#) | [Find It @ Hanyang](#)

---

166 Y. Yang, S. Liu, X. Wang, Z. Li, Y. Zhang, G. Zhang, D. Xue, J. Hu, *Adv. Funct. Mater.* 2019, **29**, 1900411.

[Web of Science®](#) | [Google Scholar](#) | [Find It @ Hanyang](#)

---

167 Y. Yang, S. Liu, W. Yang, Z. Li, Y. Wang, X. Wang, S. Zhang, Y. Zhang, M. Long, G. Zhang, D. Xue, J. Hu, L. Wan, *J. Am. Chem. Soc.* 2018, **140**, 4150.

[CAS](#) | [PubMed](#) | [Web of Science®](#) | [Google Scholar](#) | [Find It @ Hanyang](#)

---

168 C. Li, S. Wang, C. Li, T. Yu, N. Jia, J. Qiao, M. Zhu, D. Liu, X. Tao, *J. Mater. Chem. C* 2018, **6**, 7219.

[CAS](#) | [Web of Science®](#) | [Google Scholar](#) | [Find It @ Hanyang](#)

---

169 D. Kim, K. Park, J. H. Lee, I. S. Kwon, I. H. Kwak, J. Park, *Small* 2021, **17**, 2006310.

[CAS](#) | [Web of Science®](#) | [Google Scholar](#) | [Find It @ Hanyang](#)

---

170 J. O. Island, R. Biele, M. Barawi, J. M. Clamagirand, J. R. Ares, C. Sánchez, H. S. J. van der Zant, I. J. Ferrer, R. D'Agosta, A. Castellanos-Gomez, *Sci. Rep.* 2016, **6**, 22214.

[CAS](#) | [PubMed](#) | [Web of Science®](#) | [Google Scholar](#) | [Find It @ Hanyang](#)

---

171 Z. Zhou, M. Long, L. Pan, X. Wang, M. Zhong, M. Blei, J. Wang, J. Fang, S. Tongay, W. Hu, J. Li, Z. Wei, *ACS Nano* 2019, **12**, 12416.

[Web of Science®](#) | [Google Scholar](#) | [Find It @ Hanyang](#)

---

172 L. Li, W. Wang, P. Gong, X. Zhu, B. Deng, X. Shi, G. Gao, H. Li, T. Zhai, *Adv. Mater.* 2018, **30**, 1706771.

[Web of Science®](#) | [Google Scholar](#) | [Find It @ Hanyang](#)

---

173 S. Yang, C. Hu, M. Wu, W. Shen, S. Tongay, K. Wu, B. Wei, Z. Sun, C. Jiang, L. Huang, Z. Wang, *ACS Nano* 2018, **12**, 8798.

[CAS](#) | [PubMed](#) | [Web of Science®](#) | [Google Scholar](#) | [Find It @ Hanyang](#)

---

174 L. Tong, X. Huang, P. Wang, L. Ye, M. Peng, L. An, Q. Sun, Y. Zhang, G. Yang, Z. Li, F. Zhong, F. Wang, Y. Wang, M. Motlag, W. Wu, G. J. Cheng, W. Hu, *Nat. Commun.* 2020, **11**, 2308.

[CAS](#) | [PubMed](#) | [Web of Science®](#) | [Google Scholar](#) | [Find It @ Hanyang](#)

---

175 Y. Pan, Q. Zhao, F. Gao, M. Dai, W. Gao, T. Zheng, S. Su, J. Li, H. Chen, *ACS Appl. Mater. Interfaces* 2022, **14**, 21383.

[CAS](#) | [PubMed](#) | [Web of Science®](#) | [Google Scholar](#) | [Find It @ Hanyang](#)

---

176 Z. Guo, R. Cao, H. Wang, X. Zhang, F. Meng, X. Chen, S. Gao, D. Sang, T. H. Nguyen, A. Duong, J. Zhao, Y. Zeng, S. Cho, B. Zhao, P. Tan, H. Zhang, D. Fan, *Natl. Sci. Rev.* 2021, **9**, nwab098.

[PubMed](#) | [Web of Science®](#) | [Google Scholar](#) | [Find It @ Hanyang](#)

---

177 S. Wang, Z. Yang, D. Wang, C. Tan, L. Yang, Z. Wang, *ACS Appl. Mater. Interfaces* 2023, **15**, 3357.

[CAS](#) | [PubMed](#) | [Web of Science®](#) | [Google Scholar](#) | [Find It @ Hanyang](#)

---

178 J. Ahn, K. Ko, J. Kyhm, H. Ra, H. Bae, S. Hong, D. Kim, J. Jang, T. W. Kim, S. Choi, J. Kang, N. Kwon, S. Park, B. Ju, T. Poon, M. Park, S. Im, D. K. Hwang, *ACS Nano* 2022, **15**, 17917.

[Web of Science®](#) | [Google Scholar](#) | [Find It @ Hanyang](#)

---

179 H. Ni, M. Li, Y. Hu, C. Mao, L. Xue, H. Zeng, Z. Yan, Y. Wu, C. Zheng, *J. Phys. Chem. Solids* 2019, **131**, 223.

[CAS](#) | [Web of Science®](#) | [Google Scholar](#) | [Find It @ Hanyang](#)

---

180 Y. Gao, J. Liao, H. Chen, H. Ning, Q. Wu, Z. Li, Z. Wang, X. Zhang, M. Shao, Y. Yu, *Adv. Sci.* 2022, **10**, 2204727.

[Google Scholar](#) | [Find It @ Hanyang](#)

---

181 S. Wu, Y. Chen, X. Wang, H. Jiao, Q. Zhao, X. Huang, X. Tai, Y. Zhou, H. Chen, X. Wang, S. Huang, H. Yan, T. Lin, H. Shen, W. Hu, X. Meng, J. Chu, J. Wang, *Nat. Commun.* 2022, **13**, 3198.

[PubMed](#) | [Web of Science®](#) | [Google Scholar](#) | [Find It @ Hanyang](#)

---

182 J. Chen, M. Badioli, P. Alonso-González, S. Thongrattanasiri, F. Huth, J. Osmond, M. Spasenović, A. Centeno, A. Pesquera, P. Godignon, A. Z. Elorza, N. Camara, F. J. G. de Abajo, R. Hillenbrand, F. H. L. Koppens, *Nature* 2012, **487**, 77.

[CAS](#) | [PubMed](#) | [Web of Science®](#) | [Google Scholar](#) | [Find It @ Hanyang](#)

---

183 S. Dai, Z. Fei, Q. Ma, A. S. Rodin, M. Wagner, A. S. Mcleod, M. K. Liu, W. Gannett, W. Regan, K. Watanabe, T. Taniguchi, M. Thiemens, G. Dominguez, A. H. Castro Neto, A. Zettl, F. Keilmann, P. Jarillo-Herrero, M. M. Fogler, D. N. Basov, *Science* 2014, **343**, 1125.

[CAS](#) | [PubMed](#) | [Web of Science®](#) | [Google Scholar](#) | [Find It @ Hanyang](#)

---

184 P. Cristofolini, G. Christmann, S. I. Tsintzos, G. Deligeorgis, G. Konstantinidis, Z. Hatzopoulos, P. G. Savvidis, J. J. Baumberg, *Science* 2012, **336**, 704.

[CAS](#) | [PubMed](#) | [Web of Science®](#) | [Google Scholar](#) | [Find It @ Hanyang](#)

---

185 E. Ozbay, *Science* 2006, **311**, 189.

[CAS](#) | [PubMed](#) | [Web of Science®](#) | [Google Scholar](#) | [Find It @ Hanyang](#)

---

186 J. Gu, B. Chakraborty, M. Khatoniar, V. M. Menon, *Nat. Nanotechnol.* 2019, **14**, 1024.

[CAS](#) | [PubMed](#) | [Web of Science®](#) | [Google Scholar](#) | [Find It @ Hanyang](#)

---

187 A. Woessner, Y. Gao, I. Torre, M. B. Lundeberg, C. Tan, K. Watanabe, T. Taniguchi, R. Hillenbrand, J. Hone, M. Polini, F. H. L. Koppens, *Nat. Photonics* 2017, **11**, 421.

[CAS](#) | [Web of Science®](#) | [Google Scholar](#) | [Find It @ Hanyang](#)

---

188 S. Huang, C. Wang, Y. Xie, B. Yu, H. Yan, *Phot. Insights* 2023, **2**, R03.

[Google Scholar](#) | [Find It @ Hanyang](#)

---

189 P. Li, I. Dolado, F. J. Alfaro-Mozaz, F. Casanova, L. E. Hueso, S. Liu, J. H. Edgar, A. Y. Nikitin, S. Vélez, R. Hillenbrand, *Science* 2018, **359**, 892.

[CAS](#) | [PubMed](#) | [Web of Science®](#) | [Google Scholar](#) | [Find It @ Hanyang](#)

---

190 W. Ma, B. Shabbir, Q. Ou, Y. Dong, H. Chen, P. Li, X. Zhang, Y. Lu, Q. Bao, *InfoMat* 2020, **2**, 777.

[CAS](#) | [Web of Science®](#) | [Google Scholar](#) | [Find It @ Hanyang](#)

---

191 C. Wang, S. Huang, Q. Xing, Y. Xie, C. Song, F. Wang, H. Yan, *Nat. Commun.* 2020, **11**, 1158.

[CAS](#) | [PubMed](#) | [Web of Science®](#) | [Google Scholar](#) | [Find It @ Hanyang](#)

---

192 W. Ma, P. Alonso-González, S. Li, A. Y. Nikitin, J. Yuan, J. Martín-Sánchez, J. Taboada-Gutiérrez, I. Amenabar, P. Li, S. Vélez, C. Tollan, Z. Dai, Y. Zhang, S. Sriram, K. Kalantar-Zadeh, S. Lee, R. Hillenbrand, Q. Bao, *Nature* 2018, **562**, 557.

[CAS](#) | [PubMed](#) | [Web of Science®](#) | [Google Scholar](#) | [Find It @ Hanyang](#)

---

193 J. Lv, Y. Wu, J. Liu, Y. Gong, G. Si, G. Hu, Q. Zhang, Y. Zhang, J. Tang, M. S. Fuhrer, H. Chen, S. A. Maier, C. Qiu, Q. Ou, *Nat. Commun.* 2023, **14**, 3894.

[CAS](#) | [PubMed](#) | [Google Scholar](#) | [Find It @ Hanyang](#)

---

194 Q. Zhang, Q. Ou, G. Si, G. Hu, S. Dong, Y. Chen, J. Ni, C. Zhao, M. S. Fuhrer, Y. Yang, A. Alù, R. Hillenbrand, C. Qiu, *Sci. Adv.* 2022, **8**, eabn9774.

[CAS](#) | [PubMed](#) | [Web of Science®](#) | [Google Scholar](#) | [Find It @ Hanyang](#)

---

195 X. Guo, W. Lyu, T. Chen, Y. Luo, C. Wu, B. Yang, Z. Sun, F. J. G. de Abajo, X. Yang, Q. Dai, *Adv. Mater.* 2020, **35**, 2201856.

[Google Scholar](#) | [Find It @ Hanyang](#)

---

196 E. Orgiu, J. George, J. A. Hutchison, E. Devaux, J. F. Dayen, B. Doudin, F. Stellacci, C. Genet, J. Schachenmayer, C. Genes, G. Pupillo, P. Samorì, T. W. Ebbesen, *Nat. Mater.* 2015, **14**, 1123.

[CAS](#) | [PubMed](#) | [Web of Science®](#) | [Google Scholar](#) | [Find It @ Hanyang](#)

---

197 M. Freitag, T. Low, W. Zhu, H. Yan, F. Xia, P. Avouris, *Nat. Commun.* 2013, **4**, 1951.

[CAS](#) | [PubMed](#) | [Web of Science®](#) | [Google Scholar](#) | [Find It @ Hanyang](#)

---

198 H. Yan, X. Li, B. Chandra, G. Tulevski, Y. Wu, M. Freitag, W. Zhu, P. Avouris, F. Xia, *Nat. Nanotechnol.* 2012, **7**, 330.

[CAS](#) | [PubMed](#) | [Web of Science®](#) | [Google Scholar](#) | [Find It @ Hanyang](#)

---

199 L. Ju, B. Geng, J. Horng, C. Girit, M. Martin, Z. Hao, H. A. Bechtel, X. Liang, A. Zettl, Y. R. Shen, F. Wang, *Nat. Nanotechnol.* 2011, **6**, 630.

[CAS](#) | [PubMed](#) | [Web of Science®](#) | [Google Scholar](#) | [Find It @ Hanyang](#)

---

200 H. Zhang, B. Abhiraman, Q. Zhang, J. Miao, K. Jo, S. Roccasacca, M. W. Knight, A. R. Davoyan, D. Jariwala, *Nat. Commun.* 2020, **11**, 3552.

[CAS](#) | [PubMed](#) | [Web of Science®](#) | [Google Scholar](#) | [Find It @ Hanyang](#)

---

201 D. C. Flanders, *Appl. Phys. Lett.* 1983, **42**, 492.

[CAS](#) | [Web of Science®](#) | [Google Scholar](#) | [Find It @ Hanyang](#)

---

202 S. Yang, M. L. Cooper, P. R. Bandaru, S. Mookherjea, *Opt. Express* 2008, **16**, 8306.

[PubMed](#) | [Web of Science®](#) | [Google Scholar](#) | [Find It @ Hanyang](#)

---

203 T. Zou, B. Zhao, W. Xin, F. Wang, H. Xie, Y. Li, Y. Shan, K. Li, Y. Sun, J. Yang, *Nano. Res.* 2021, **15**, 4490.

[Web of Science®](#) | [Google Scholar](#) | [Find It @ Hanyang](#)



---

204 C. J. Powell, *J. Nucl. Energy, Part C Plasma Phys.* 1961, **2**, 57.

[Google Scholar](#) | [Find It @ Hanyang](#)

---

205 T. W. Ebbesen, H. J. Lezec, H. F. Ghaemi, T. Thio, P. A. Wolff, *Nature* 1998, **391**, 667.

[CAS](#) | [Web of Science®](#) | [Google Scholar](#) | [Find It @ Hanyang](#)

---

206 F. Afshinmanesh, J. S. White, W. Cai, M. L. Brongersma, *Nanophotonics* 2012, **1**, 125.

[CAS](#) | [Web of Science®](#) | [Google Scholar](#) | [Find It @ Hanyang](#)

---

207 G. P. Nordin, J. T. Meier, P. C. Deguzman, M. W. Jones, *J. Opt. Soc. Am. A* 1999, **16**, 1168.

[Web of Science®](#) | [Google Scholar](#) | [Find It @ Hanyang](#)

---

208 Y. Hu, X. Wang, X. Luo, X. Ou, L. Li, Y. Chen, P. Yang, S. Wang, H. Duan, *Nanophotonics* 2020, **9**, 3755.

[Web of Science®](#) | [Google Scholar](#) | [Find It @ Hanyang](#)

---

209 M. Dai, C. Wang, B. Qiang, F. Wang, M. Ye, S. Han, Y. Luo, Q. Wang, *Nat. Commun.* 2022, **13**, 4560.

[CAS](#) | [PubMed](#) | [Web of Science®](#) | [Google Scholar](#) | [Find It @ Hanyang](#)

---

210 Q. Bao, H. Zhang, B. Wang, Z. Ni, C. H. Y. X. Lim, Y. Wang, D. Tang, K. P. Loh, *Nat. Photonics* 2011, **5**, 411.

[CAS](#) | [Web of Science®](#) | [Google Scholar](#) | [Find It @ Hanyang](#)

---

211 W. Xin, Z. Liu, Q. Sheng, M. Feng, L. Huang, P. Wang, W. Jiang, F. Xing, Y. Liu, J. Tian, *Opt. Express* 2014, **22**, 10239.

[CAS](#) | [PubMed](#) | [Web of Science®](#) | [Google Scholar](#) | [Find It @ Hanyang](#)

---

212 M. Liu, X. Yin, E. Ulin-Avila, B. Geng, T. Zentgraf, L. Ju, F. Wang, X. Zhang, *Nature* 2011, **474**, 64.

[CAS](#) | [PubMed](#) | [Web of Science®](#) | [Google Scholar](#) | [Find It @ Hanyang](#)

---

---

213 C. Li, R. Tian, R. Yi, S. Hu, Y. Chen, Q. Yuan, X. Zhang, Y. Liu, Y. Hao, X. Gan, J. Zhao, *ACS Photonics* 2021, **8**, 2431.

[CAS](#) | [Web of Science®](#) | [Google Scholar](#) | [Find It @ Hanyang](#)

---

214 X. Wang, Z. Cheng, K. Xu, H. K. Tsang, J. Xu, *Nat. Photonics* 2013, **7**, 888.

[CAS](#) | [Web of Science®](#) | [Google Scholar](#) | [Find It @ Hanyang](#)

---

215 N. Youngblood, C. Chen, S. J. Koester, M. Li, *Nat. Photonics* 2015, **9**, 247.

[CAS](#) | [Web of Science®](#) | [Google Scholar](#) | [Find It @ Hanyang](#)

---

216 F. Xing, W. Xin, W. Jiang, Z. Liu, J. Tian, *Appl. Phys. Lett.* 2015, **107**, 163110.

[CAS](#) | [Web of Science®](#) | [Google Scholar](#) | [Find It @ Hanyang](#)

---

217 W. Xin, X. Chen, Z. Liu, W. Jiang, X. Gao, X. Jiang, Y. Chen, J. Tian, *Adv. Opt. Mater.* 2016, **4**, 1703.

[CAS](#) | [Web of Science®](#) | [Google Scholar](#) | [Find It @ Hanyang](#)

---

218 W. Xin, H. Jiang, T. Sun, X. Gao, S. Chen, B. Zhao, J. Yang, Z. Liu, J. Tian, C. Guo, *Nano Mater. Sci.* 2019, **1**, 304.

[Google Scholar](#) | [Find It @ Hanyang](#)

---

219 R. A. Hann, G. Read, D. R. Rosseinsky, P. Wassell, *Nat. Phys. Sci.* 1973, **244**, 126.

[CAS](#) | [Web of Science®](#) | [Google Scholar](#) | [Find It @ Hanyang](#)

---

220 V. M. Fridkin, E. P. Efremova, B. H. Karimov, V. A. Kuznezov, I. P. Kuzmina, A. N. Lobachev, V. G. Lazarev, A. J. Rodin, *Appl. Phys.* 1981, **25**, 77.

[CAS](#) | [Web of Science®](#) | [Google Scholar](#) | [Find It @ Hanyang](#)

---

221 C. Guo, Y. Hu, G. Chen, D. Wei, L. Zhang, Z. Chen, W. Guo, H. Xu, C. N. Kuo, C. S. Lue, X. Bo, X. Wan, L. Wang, A. Politano, X. Chen, W. Lu, *Sci. Adv.* 2020, **6**, eabb6500.

[CAS](#) | [PubMed](#) | [Web of Science®](#) | [Google Scholar](#) | [Find It @ Hanyang](#)

---

222 S. Dhara, E. J. Mele, R. Agarwal, *Science* 2015, **349**, 726.

[CAS](#) | [PubMed](#) | [Web of Science®](#) | [Google Scholar](#) | [Find It @ Hanyang](#)

---

223 P. Král, E. J. Mele, D. Tománek, *Phys. Rev. Lett.* 2000, **85**, 1512.

[CAS](#) | [PubMed](#) | [Web of Science®](#) | [Google Scholar](#) | [Find It @ Hanyang](#)

---

224 H. Yuan, X. Wang, B. Lian, H. Zhang, X. Fang, B. Shen, G. Xu, Y. Xu, S. Zhang, H. Y. Hwang, Y. Cui, *Nat. Nanotechnol.* 2014, **9**, 851.

[CAS](#) | [PubMed](#) | [Web of Science®](#) | [Google Scholar](#) | [Find It @ Hanyang](#)

---

225 F. de Juan, A. G. Grushin, T. Morimoto, J. E. Moore, *Nat. Commun.* 2017, **8**, 15995.

[PubMed](#) | [Web of Science®](#) | [Google Scholar](#) | [Find It @ Hanyang](#)

---

226 Q. Ma, S. Xu, C. Chan, C. Zhang, G. Chang, Y. Lin, W. Xie, T. Palacios, H. Lin, S. Jia, P. A. Lee, P. Jarillo-Herrero, N. Gedik, *Nat. Phys.* 2017, **13**, 842.

[CAS](#) | [Web of Science®](#) | [Google Scholar](#) | [Find It @ Hanyang](#)

---

227 Y. Gao, Y. Zhang, D. Xiao, *Phys. Rev. Lett.* 2020, **124**, 077401.

[CAS](#) | [PubMed](#) | [Web of Science®](#) | [Google Scholar](#) | [Find It @ Hanyang](#)

---

228 Z. Ji, W. Liu, S. Krylyuk, X. Fan, Z. Zhang, A. Pan, L. Feng, A. Davydov, R. Agarwal, *Science* 2020, **368**, 763.

[CAS](#) | [PubMed](#) | [Web of Science®](#) | [Google Scholar](#) | [Find It @ Hanyang](#)

---

229 J. Lai, J. Ma, Z. Fan, X. Song, P. Yu, Z. Liu, P. Zhang, Y. Shi, J. Cheng, D. Sun, *Adv. Mater.* 2022, **34**, 2201229.

[CAS](#) | [Web of Science®](#) | [Google Scholar](#) | [Find It @ Hanyang](#)

---

230 H. M. Barlow, *Proc. IRE* 1958, **46**, 1411.

[Web of Science®](#) | [Google Scholar](#) | [Find It @ Hanyang](#)

---

231 A. M. Danishevskii, A. A. Kastalskii, S. M. Ryvkin, I. D. Yaroshetskii, *Sov. Phys. JETP* 1970, **31**, 544.

[Google Scholar](#) | [Find It @ Hanyang](#)

---

232 S. Luryi, *Phys. Rev. Lett.* 1987, **58**, 2263.

[CAS](#) | [PubMed](#) | [Web of Science®](#) | [Google Scholar](#) | [Find It @ Hanyang](#)

---

233 V. A. Shalygin, M. D. Moldavskaya, S. N. Danilov, I. I. Farbshtein, L. E. Golub, *Phys. Rev. B* 2016, **93**, 045207.

[Web of Science®](#) | [Google Scholar](#) | [Find It @ Hanyang](#)

---

234 M. V. Entin, L. I. Magarill, D. L. Shepelyansky, *Phys. Rev. B* 2010, **81**, 165441.

[CAS](#) | [Web of Science®](#) | [Google Scholar](#) | [Find It @ Hanyang](#)

---

235 G. M. Mikheev, A. G. Nasibulin, R. G. Zonov, A. Kaskela, E. I. Kauppinen, *Nano Lett.* 2012, **12**, 77.

[CAS](#) | [PubMed](#) | [Web of Science®](#) | [Google Scholar](#) | [Find It @ Hanyang](#)

---

236 H. Plank, L. E. Golub, S. Bauer, V. V. Bel'kov, T. Herrmann, P. Olbrich, M. Eschbach, L. Plucinski, C. M. Schneider, J. Kampmeier, M. Lanius, G. Mussler, D. Grützmacher, S. D. Ganichev, *Phys. Rev. B* 2016, **93**, 125434.

[CAS](#) | [Web of Science®](#) | [Google Scholar](#) | [Find It @ Hanyang](#)

---

237 L. Shi, D. Zhang, K. Chang, J. C. W. Song, *Phys. Rev. Lett.* 2021, **126**, 197402.

[CAS](#) | [PubMed](#) | [Web of Science®](#) | [Google Scholar](#) | [Find It @ Hanyang](#)

---

238 Y. Xiong, L. Shi, J. C. W. Song, *Phys. Rev. B* 2022, **106**, 205423.

[CAS](#) | [Google Scholar](#) | [Find It @ Hanyang](#)

---

239 Y. Dang, X. Tao, *Matter* 2022, **5**, 2659.

[CAS](#) | [Google Scholar](#) | [Find It @ Hanyang](#)

---

240 Y. Peng, X. Liu, Z. Sun, C. Ji, L. Li, Z. Wu, S. Wang, Y. Yao, M. Hong, J. Luo, *Angew. Chem., Int. Ed.* 2020, **59**, 3933.

[CAS](#) | [PubMed](#) | [Web of Science®](#) | [Google Scholar](#) | [Find It @ Hanyang](#)

---

241 R. P. Tiwari, B. Birajdar, R. K. Ghosh, *Phys. Rev. B* 2020, **101**, 235448.

[CAS](#) | [Web of Science®](#) | [Google Scholar](#) | [Find It @ Hanyang](#)

---

242 D. S. Knoche, M. Steimecke, Y. Yun, L. Muehlenbein, A. Bhatnagar, *Nat. Commun.* 2021, **12**, 282.

[CAS](#) | [PubMed](#) | [Web of Science®](#) | [Google Scholar](#) | [Find It @ Hanyang](#)

---

243 A. Mathew, V. K. Pulikodan, M. A. G. Namboothiry, *Appl. Phys. Lett.* 2022, **121**, 233102.

[CAS](#) | [Google Scholar](#) | [Find It @ Hanyang](#)

---

244 T. Akamatsu, T. Ideue, L. Zhou, Y. Dong, S. Kitamura, M. Yoshii, D. Yang, M. Onga, Y. Nakagawa, K. Watanabe, T. Taniguchi, J. Laurienzo, J. Huang, Z. Ye, T. Morimoto, H. Yuan, Y. Iwasa, *Science* 2021, **372**, 68.

[CAS](#) | [PubMed](#) | [Web of Science®](#) | [Google Scholar](#) | [Find It @ Hanyang](#)

---

245 Z. Hu, L. Zhang, A. Chakraborty, G. D'Olimpio, J. Fujii, A. Ge, Y. Zhou, C. Liu, A. Agarwal, I. Vobornik, D. Farias, C. Kuo, C. S. Lue, A. Politano, S. Wang, W. Hu, X. Chen, W. Lu, L. Wang, *Adv. Mater.* 2023, **35**, 2209557.

[CAS](#) | [Web of Science®](#) | [Google Scholar](#) | [Find It @ Hanyang](#)

---

246 M. D. Ward, W. Shi, N. Gasparini, J. Nelson, J. Wade, M. J. Fuchter, *J. Mater. Chem. C* 2022, **10**, 10452.

[CAS](#) | [PubMed](#) | [Web of Science®](#) | [Google Scholar](#) | [Find It @ Hanyang](#)

---

247 J. Cai, W. Zhang, L. Xu, C. Hao, W. Ma, M. Sun, X. Wu, X. Qin, F. M. Colombari, A. F. de Moura, J. Xu, M. C. Silva, E. B. Carneiro-Neto, W. R. Gomes, R. A. L. Vallée, E. C. Pereira, X. Liu, C. Xu, R. Klajn, N. A. Kotov, H. Kuang, *Nat. Nanotechnol.* 2022, **17**, 408.

[CAS](#) | [PubMed](#) | [Web of Science®](#) | [Google Scholar](#) | [Find It @ Hanyang](#)

---

248 S. D. Namgung, R. M. Kim, Y. Lim, J. W. Lee, N. H. Cho, H. Kim, J. Huh, H. Rhee, S. Nah, M. Song, J. Kwon, K. T. Nam, *Nat. Commun.* 2022, **13**, 5081.

[CAS](#) | [PubMed](#) | [Web of Science®](#) | [Google Scholar](#) | [Find It @ Hanyang](#)

---

249 Y. Yang, R. C. da Costa, M. J. Fuchter, A. J. Campbell, *Nat. Photonics* 2013, **7**, 634.

[CAS](#) | [Web of Science®](#) | [Google Scholar](#) | [Find It @ Hanyang](#)

---

250 Z. Qiu, C. Ju, L. Frédéric, Y. Hu, D. Schollmeyer, G. Pieters, K. Müllen, A. Narita, *J. Am. Chem. Soc.* 2021, **143**, 4661.

[CAS](#) | [PubMed](#) | [Web of Science®](#) | [Google Scholar](#) | [Find It @ Hanyang](#)

---

251 A. Ishii, T. Miyasaka, *Sci. Adv.* 2020, **6**, eabd3274.

[CAS](#) | [PubMed](#) | [Web of Science®](#) | [Google Scholar](#) | [Find It @ Hanyang](#)

---

252 V. K. Valev, J. J. Baumberg, C. Sibia, T. Verbiest, *Adv. Mater.* 2013, **25**, 2517.

[CAS](#) | [PubMed](#) | [Web of Science®](#) | [Google Scholar](#) | [Find It @ Hanyang](#)

---

253 Y. Intaravanne, X. Chen, *Nanophotonics* 2020, **9**, 1003.

[Web of Science®](#) | [Google Scholar](#) | [Find It @ Hanyang](#)

---

254 Y. Bu, X. Ren, J. Zhou, Z. Zhang, J. Deng, H. Xu, R. Xie, T. Li, W. Hu, X. Guo, W. Lu, X. Chen, *Light: Sci. Appl.* 2023, **12**, 176.

[CAS](#) | [PubMed](#) | [Google Scholar](#) | [Find It @ Hanyang](#)

---

255 P. Seifert, K. Vaklinova, S. Ganichev, K. Kern, M. Burghard, A. W. Holleitner, *Nat. Commun.* 2018, **9**, 331.

[PubMed](#) | [Web of Science®](#) | [Google Scholar](#) | [Find It @ Hanyang](#)

---

256 J. Wei, Y. Li, L. Wang, W. Liao, B. Dong, C. Xu, C. Zhu, K. Ang, C. Qiu, C. Lee, *Nat. Commun.* 2020, **11**, 6404.

[CAS](#) | [PubMed](#) | [Web of Science®](#) | [Google Scholar](#) | [Find It @ Hanyang](#)

---

257 J. Wei, C. Xu, B. Dong, C. Qiu, C. Lee, *Nat. Photonics* 2021, **15**, 614.

[CAS](#) | [Web of Science®](#) | [Google Scholar](#) | [Find It @ Hanyang](#)

---

258 J. Wei, Y. Chen, Y. Li, W. Li, J. Xie, C. Lee, K. S. Novoselov, C. Qiu, *Nat. Photonics* 2023, **17**, 171.

[CAS](#) | [Web of Science®](#) | [Google Scholar](#) | [Find It @ Hanyang](#)

---

259 C. Fang, J. Li, B. Zhou, D. Li, *Nano Lett.* 2021, **21**, 6156.

[CAS](#) | [PubMed](#) | [Web of Science®](#) | [Google Scholar](#) | [Find It @ Hanyang](#)

---

260 X. Sun, G. Adamo, M. Eginligil, H. N. S. Krishnamoorthy, N. I. Zheludev, C. Soci, *Sci. Adv.* 2021, **7**, eabe5748.

[CAS](#) | [PubMed](#) | [Web of Science®](#) | [Google Scholar](#) | [Find It @ Hanyang](#)

---

261 F. Xing, G. Ji, Z. Li, W. Zhong, F. Wang, Z. Liu, W. Xin, J. Tian, *Mater. Horiz.* 2023, **10**, 722.

[CAS](#) | [PubMed](#) | [Web of Science®](#) | [Google Scholar](#) | [Find It @ Hanyang](#)

---

262 Z. Zheng, Y. Song, Y. Shan, W. Xin, J. Cheng, *Phys. Rev. B* 2022, **105**, 085407.

[CAS](#) | [Google Scholar](#) | [Find It @ Hanyang](#)

---

263 Y. Ge, M. Zhang, L. Wang, L. Meng, J. Tang, Y. Chen, L. Wang, H. Zhong, *Adv. Opt. Mater.* 2019, **7**, 1900330.

[Web of Science®](#) | [Google Scholar](#) | [Find It @ Hanyang](#)

---

264 J. W. John, V. Dhyani, S. Singh, A. Jakhar, A. Sarkar, S. Das, S. K. Ray, *Nanotechnology* 2021, **32**, 315205.

[CAS](#) | [Web of Science®](#) | [Google Scholar](#) | [Find It @ Hanyang](#)

---

265 R. Ghosh, H. I. Lin, Y. S. Chen, M. Singh, Z. L. Yen, S. Chiu, H. Y. Lin, K. P. Bera, Y. Liao, M. Hofmann, Y. P. Hsieh, *Small* 2020, **16**, 2003944.

[CAS](#) | [Web of Science®](#) | [Google Scholar](#) | [Find It @ Hanyang](#)

---

266 D. Ghoshal, T. Wang, H. Tsai, S. Chang, M. Crommie, N. Koratkar, S. Shi, *Adv. Opt. Mater.* 2019, **7**, 1900039.

[Web of Science®](#) | [Google Scholar](#) | [Find It @ Hanyang](#)

---

267 Y. Zhou, L. Han, Q. Song, W. Gao, M. Yang, Z. Zheng, L. Huang, J. Yao, J. Li, *Sci. China Mater.* 2022, **65**, 732.

[CAS](#) | [Web of Science®](#) | [Google Scholar](#) | [Find It @ Hanyang](#)

---

268 D. Wu, C. Jia, F. Shi, L. Zeng, P. Lin, L. Dong, Z. Shi, Y. Tian, X. Li, J. Jie, *J. Mater. Chem. A* 2020, **8**, 3632.

[CAS](#) | [Web of Science®](#) | [Google Scholar](#) | [Find It @ Hanyang](#)

---

269 Y. Niu, R. Frisenda, E. Flores, J. R. Ares, W. Jiao, D. P. de Lara, C. Sánchez, R. Wang, I. J. Ferrer, A. Castellanos-Gomez, *Adv. Opt. Mater.* 2018, **6**, 1800351.

[Web of Science®](#) | [Google Scholar](#) | [Find It @ Hanyang](#)

---

270 Y. Liu, B. N. Shivananju, Y. Wang, Y. Zhang, W. Yu, S. Xiao, T. Sun, W. Ma, H. Mu, S. Lin, H. Zhang, Y. Lu, C. Qiu, S. Li, Q. Bao, *ACS Appl. Mater. Interfaces* 2017, **9**, 36137.

[CAS](#) | [PubMed](#) | [Web of Science®](#) | [Google Scholar](#) | [Find It @ Hanyang](#)

---

271 S. Zhao, J. Wu, K. Jin, H. Ding, T. Li, C. Wu, N. Pan, X. Wang, *Adv. Funct. Mater.* 2018, **28**, 1802011.

[Web of Science®](#) | [Google Scholar](#) | [Find It @ Hanyang](#)

---

272 X. Li, X. Gao, B. Su, W. Xin, K. Huang, X. Jiang, Z. Liu, J. Tian, *Adv. Mater. Interfaces* 2018, **5**, 1800960.

[Web of Science®](#) | [Google Scholar](#) | [Find It @ Hanyang](#)

---

273 B. Su, X. Li, X. Jiang, W. Xin, K. Huang, D. Li, H. Guo, Z. Liu, J. Tian, *ACS Appl. Mater. Interfaces* 2018, **10**, 35615.

[CAS](#) | [PubMed](#) | [Web of Science®](#) | [Google Scholar](#) | [Find It @ Hanyang](#)

---

274 C. Jia, D. Wu, E. Wu, J. Guo, Z. Zhao, Z. Shi, T. Xu, X. Huang, Y. Tian, X. Li, *J. Mater. Chem. C* 2019, **7**, 3817.

[CAS](#) | [Web of Science®](#) | [Google Scholar](#) | [Find It @ Hanyang](#)

---

275 L. Zeng, Q. Chen, Z. Zhang, D. Wu, H. Yuan, Y. Li, W. Qarony, S. P. Lau, L. Luo, Y. H. Tsang, *Adv. Sci.* 2019, **6**, 1901134.

[CAS](#) | [Google Scholar](#) | [Find It @ Hanyang](#)

---

276 J. Xiong, Y. Sun, L. Wu, W. Wang, W. Gao, N. Huo, J. Li, *Adv. Opt. Mater.* 2021, **9**, 2101017.

[CAS](#) | [Web of Science®](#) | [Google Scholar](#) | [Find It @ Hanyang](#)



---

277 Z. Luo, H. Xu, W. Gao, M. Yang, Y. He, Z. Huang, J. Yao, M. Zhang, H. Dong, Y. Zhao, Z. Zheng, J. Li, *Small* 2023, **19**, 2207615.

[CAS](#) | [PubMed](#) | [Web of Science®](#) | [Google Scholar](#) | [Find It @ Hanyang](#)

---

278 D. Wu, J. Guo, J. Du, C. Xia, L. Zeng, Y. Tian, Z. Shi, Y. Tian, X. Li, Y. H. Tsang, J. Jie, *ACS Nano* 2019, **13**, 9907.

[CAS](#) | [PubMed](#) | [Web of Science®](#) | [Google Scholar](#) | [Find It @ Hanyang](#)

---

279 D. Wu, M. Xu, L. Zeng, Z. Shi, Y. Tian, X. Li, C. Shan, J. Jie, *ACS Nano* 2022, **16**, 5545.

[CAS](#) | [PubMed](#) | [Web of Science®](#) | [Google Scholar](#) | [Find It @ Hanyang](#)

---

280 S. Shi, X. Xu, D. C. Ralph, P. L. McEuen, *Nano Lett.* 2011, **11**, 1814.

[CAS](#) | [PubMed](#) | [Web of Science®](#) | [Google Scholar](#) | [Find It @ Hanyang](#)

---

281 L. Liu, Y. Liu, T. Gong, W. Huang, J. Guo, X. Zhang, S. Zhou, B. Yu, *Nanotechnology* 2019, **30**, 435205.

[CAS](#) | [PubMed](#) | [Web of Science®](#) | [Google Scholar](#) | [Find It @ Hanyang](#)

---

282 C. Li, C. Chen, Y. Liu, J. Su, D. Qi, J. He, R. Fan, Q. Cai, Q. Li, R. Peng, X. Huang, M. Wang, *Opt. Lett.* 2022, **47**, 565.

[CAS](#) | [PubMed](#) | [Web of Science®](#) | [Google Scholar](#) | [Find It @ Hanyang](#)

---

283 T. J. Echtermeyer, S. Milana, U. Sassi, A. Eiden, M. Wu, E. Lidorikis, A. C. Ferrari, *Nano Lett.* 2016, **16**, 8.

[CAS](#) | [PubMed](#) | [Web of Science®](#) | [Google Scholar](#) | [Find It @ Hanyang](#)

---

284 D. Zhang, J. Zhou, C. Liu, S. Guo, J. Deng, Q. Cai, Z. Li, Y. Zhang, W. Zhang, X. Chen, *J. Appl. Phys.* 2019, **126**, 074301.

[Web of Science®](#) | [Google Scholar](#) | [Find It @ Hanyang](#)

---

285 M. Chen, Y. Wang, Z. Zhao, *ACS Nano* 2022, **16**, 17263.

[CAS](#) | [PubMed](#) | [Web of Science®](#) | [Google Scholar](#) | [Find It @ Hanyang](#)

---

286 S. Chen, R. Cao, X. Chen, Q. Wu, Y. Zeng, S. Gao, Z. Guo, J. Zhao, M. Zhang, H. Zhang, *Adv. Mater. Interfaces* 2020, **7**, 1902179.

[CAS](#) | [Web of Science®](#) | [Google Scholar](#) | [Find It @ Hanyang](#)

---

287 B. Chen, Z. Ji, J. Zhou, Y. Yu, X. Dai, M. Lan, Y. Bu, T. Zhu, Z. Li, J. Hao, X. Chen, *Nanoscale* 2020, **12**, 11808.

[CAS](#) | [PubMed](#) | [Web of Science®](#) | [Google Scholar](#) | [Find It @ Hanyang](#)

---

288 P. K. Venuthurumilli, P. D. Ye, X. Xu, *ACS Nano* 2018, **12**, 4861.

[CAS](#) | [PubMed](#) | [Web of Science®](#) | [Google Scholar](#) | [Find It @ Hanyang](#)

---

289 M. P. van Kouwen, M. H. M. van Weert, M. E. Reimer, N. Akopian, U. Perinetti, R. E. Algra, E. P. A. M. Bakkers, L. P. Kouwenhoven, V. Zwiller, *Appl. Phys. Lett.* 2010, **97**, 113108.

[Web of Science®](#) | [Google Scholar](#) | [Find It @ Hanyang](#)

---

290 R. Ghosh, H. Lin, Y. Chen, M. Singh, Z. Yen, S. Chiu, H. Lin, K. P. Bera, Y. Liao, M. Hofmann, Y. Hsieh, Y. Chen, *Small* 2020, **16**, 2003944.

[CAS](#) | [Web of Science®](#) | [Google Scholar](#) | [Find It @ Hanyang](#)

---

291 L. Ye, P. Wang, W. Luo, F. Gong, L. Liao, T. Liu, L. Tong, J. Zang, J. Xu, W. Hu, *Nano Energy* 2017, **37**, 53.

[CAS](#) | [Web of Science®](#) | [Google Scholar](#) | [Find It @ Hanyang](#)

---

292 J. Pan, Y. Wu, X. Zhang, J. Chen, J. Wang, S. Cheng, X. Wu, X. Zhang, J. Jie, *Nat. Commun.* 2022, **13**, 6629.

[CAS](#) | [PubMed](#) | [Web of Science®](#) | [Google Scholar](#) | [Find It @ Hanyang](#)

---

293 X. Zheng, Y. Wei, X. Zhang, Z. Wei, W. Luo, X. Guo, J. Liu, G. Peng, W. Cai, H. Huang, T. Lv, C. Deng, X. Zhang, *Adv. Funct. Mater.* 2022, **32**, 2202658.

[CAS](#) | [Web of Science®](#) | [Google Scholar](#) | [Find It @ Hanyang](#)

---

294 J. Yan, X. Yang, X. Liu, C. Du, F. Qin, M. Yang, Z. Zheng, J. Li, *Adv. Sci.* 2023, **10**, 2207022.

[CAS](#) | [Google Scholar](#) | [Find It @ Hanyang](#)

---

295 Y. Xiong, Y. Wang, R. Zhu, H. Xu, C. Wu, J. Chen, Y. Ma, Y. Liu, Y. Chen, K. Watanabe, T. Taniguchi, M. Shi, X. Chen, Y. Lu, P. Zhan, Y. Hao, F. Xu, *Sci. Adv.* 2022, **8**, eabo0375.

[CAS](#) | [PubMed](#) | [Web of Science®](#) | [Google Scholar](#) | [Find It @ Hanyang](#)

---

296 Y. Chen, X. Wang, L. Huang, X. Wang, W. Jiang, Z. Wang, P. Wang, B. Wu, T. Lin, H. Shen, Z. Wei, W. Hu, X. Meng, J. Chu, J. Wang, *Nat. Commun.* 2021, **12**, 4030.

[CAS](#) | [PubMed](#) | [Web of Science®](#) | [Google Scholar](#) | [Find It @ Hanyang](#)

---

297 S. Yuan, C. Ma, E. Fetaya, T. Mueller, D. Naveh, F. Zhang, F. Xia, *Science* 2023, **379**, eade1220.

[CAS](#) | [PubMed](#) | [Google Scholar](#) | [Find It @ Hanyang](#)

## Citing Literature



[Download PDF](#)

### ABOUT WILEY ONLINE LIBRARY

[Privacy Policy](#)  
[Terms of Use](#)  
[About Cookies](#)  
[Manage Cookies](#)  
[Accessibility](#)

[Wiley Research DE&I Statement and Publishing Policies](#)  
[Developing World Access](#)

### HELP & SUPPORT

[Contact Us](#)  
[Training and Support](#)  
[DMCA & Reporting Piracy](#)

### OPPORTUNITIES

[Subscription Agents](#)  
[Advertisers & Corporate Partners](#)

### CONNECT WITH WILEY

[The Wiley Network](#)  
[Wiley Press Room](#)

Copyright © 1999-2024 John Wiley & Sons, Inc or related companies. All rights reserved, including rights for text and data mining and training of artificial technologies or similar technologies.